Politecnico di Torino
DIPARTIMENTO DI AUTOMATICA E INFORMATICA
Corso di laurea magistrale in Ingegneria Meccatronica

Elaborato di Tesi

Design of an assistive robot

Candidato:
Fabio Petracchi

Relatore:
Marcello Chiaberge

Correlatore:
Luca Carbonari

Anno Accademico 2020-2021

Summary

Introduction

As reported by the UN (1) the expected growth of the population older than 60 years is from 18.8% in 2000 to 34.2% in 2050, showing an exponential growth of the elder people in the world.
Hence an always bigger number of people will show a substantial decrease of their mobility and capability in doing daily tasks.
Moreover, an affordable aid with the daily house task will result of interest for everyone, not only the elderly.
As a matter of fact, a solution to this issue can be provided by the recent development of automation.

This Thesis offer as an answer an innovative platform for wheeled mobile robots (WMR) designed for assistive purposes.
Giving assistance inside a house concern a lot of mobility issues, because the WMR must be able not only to navigate into an indoor environment without causing any trouble but also to react rapidly to unknown modifications at the environment.
To deal with these problems it is necessary a sophisticated software capable of an accurate path planning, but it isn't sufficient.

To follow complex trajectory or react rapidly to an uncommon obstacle on the path the platform structure must be advanced enough; for example the most used actuation for assistive WMR is the simple Differential Drive, as we will see in the chapter 1, but this typology of platform has a very restricted mobility making useless a sophisticate path planning.
In this scenario, finding a modular solution could be very interesting for the market, because not only allows to design the software separately but also can be implemented for very different applications, opening many more opportunity.
In addition, it's fundamental that this platform will be as cheaper as possible in order to put this platform into production.

Chapter 1

State of the art

In this chapter will be analysed the state of the art of the Wheeled Mobile Robot (WMR).

In the section 1.1 a classification of the various kind of WMR is done. Primarily a wheel classification is carried out, then three design variables are defined: degree of manoeuvrability (δ_M), degree of mobility (δ_m) and degree of steerability (δ_s). Finally manipulating these three design variables, five different structures determined.

In the section 1.2 the differences between omni-directional and pseudo-omnidirectional WMR is analysed in order to determine pros and cons of these two structures.

Inside the section 1.3 there is a view of what actually the market offers in terms of WMR designed specifically for assistive purpose.

1.1 Classification

First, a WMR classification with respect to kinematic and dynamic properties is essential. Such analysis can be found in (2), where three design variables are defined: degree of manoeuvrability (δ_M), degree of mobility (δ_m) and degree of steerability (δ_s).

Such variables depend only on the type and number of wheels (and if they are on the same axis) and not on other structural properties of the platform.

There are essentially two kind of wheels: **Conventional Wheel** and **Omni-wheels.**

For a Conventional wheel the contact between wheel and ground is supposed to satisfy pure rolling condition without slip. They can be **Fixed, Centered orientable** or **Off-centered** (Castor).

For an Omni-wheel instead, only one component of the velocity of the contact point is supposed to be equal to zero. Its direction is a priori arbitrary but fixed with respect to the orientation of the wheel.

Here it is shown the expressions of the constraints for the various kind of wheel:

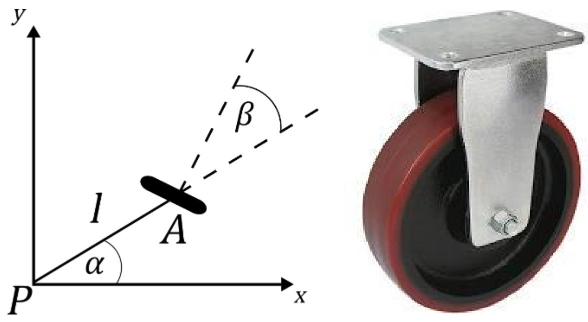

Figure 1.1 Fixed and Centered Orientable Wheel

- **Fixed Wheels:**

$$[-\sin(\alpha+\beta) \quad \cos(\alpha+\beta) \quad lcos\beta]R(\theta)\dot{x} + r\dot{\varphi} = 0$$
$$[\cos(\alpha+\beta) \quad \sin(\alpha+\beta) \quad lsin\beta]R(\theta)\dot{x} = 0$$

Where ***P*** is the origin point of the r.f. attached to the platform, ***A*** is the centre of the wheel and is characterized using polar coordinates by the distance $\overline{\boldsymbol{PA}} = \boldsymbol{l}$ and the angle $\boldsymbol{\alpha}$. The orientation of the plane of the wheel is characterized by the fixed angle $\boldsymbol{\beta}$. The rotation angle of the wheel around its axis is denoted by $\boldsymbol{\varphi}(\boldsymbol{t})$ and the radius is ***r***.

- **Centered orientable Wheels:**

$$[-\sin(\alpha+\beta) \quad \cos(\alpha+\beta) \quad lcos\beta]R(\theta)\dot{x} + r\dot{\varphi} = 0$$
$$[\cos(\alpha+\beta) \quad \sin(\alpha+\beta) \quad lsin\beta]R(\theta)\dot{x} = 0$$

Where ***P*** is the origin point of the r.f. attached to the platform, ***A*** is characterized using polar coordinates by the distance $\overline{\boldsymbol{PA}} = \boldsymbol{l}$ and the angle $\boldsymbol{\alpha}$. The orientation of the plane of the wheel is characterized by the angle $\boldsymbol{\beta(t)}$. The rotation angle of the wheel around its axis is denoted by $\boldsymbol{\varphi(t)}$ and the radius is ***r***.

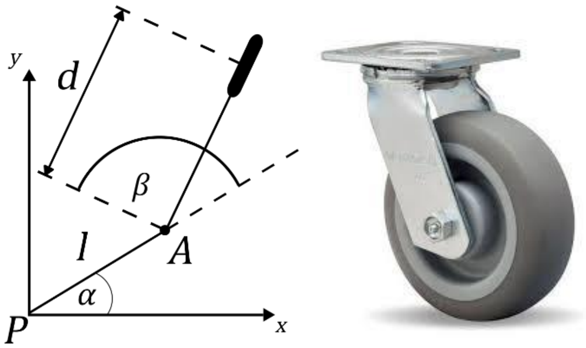

Figure 1.2 Off-centered Wheels

- **Off-centered Wheels:**

$$[-\sin(\alpha+\beta) \quad \cos(\alpha+\beta) \quad lcos\beta]R(\theta)\dot{x} + r\dot{\varphi} = 0$$
$$[\cos(\alpha+\beta) \quad \sin(\alpha+\beta) \quad d + lsin\beta]R(\theta)\dot{x} + d\dot{\beta} = 0$$

Where ***P*** is the origin point of the r.f. attached to the platform, ***B*** is the centre of the wheel and is connected to the frame by a rigid rod $\overline{\boldsymbol{AB}}$ of constant length ***d*** which can rotate of an angle $\boldsymbol{\beta(t)}$ around a fixed axis at point ***A***. This point is the centre of the wheel and is characterized using polar coordinates by the distance $\overline{\boldsymbol{PA}} = \boldsymbol{l}$ and the angle $\boldsymbol{\alpha}$. The orientation of the plane of the wheel is aligned along $\overline{\boldsymbol{AB}}$. The rotation angle of the wheel around its axis is denoted by $\boldsymbol{\varphi(t)}$ and the radius is ***r***.

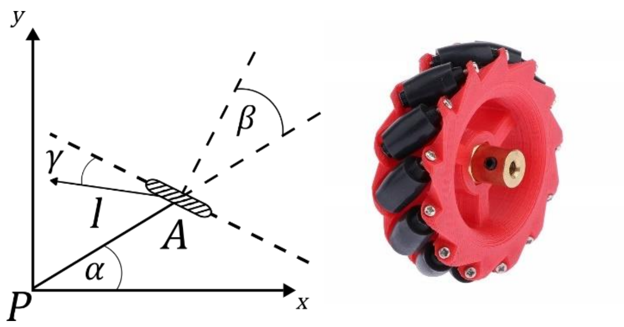

Figure 1.3 Omni-wheel

- **Omni-Wheels:**

$$[-\sin(\alpha+\beta+\gamma) \quad \cos(\alpha+\beta+\gamma) \quad l\cos(\beta+\gamma)]R(\theta)\dot{x} + r\dot{\varphi}\cos\gamma = 0$$

Where ***P*** is the origin point of the r.f. attached to the platform, ***A*** is the centre of the wheel and is characterized using polar coordinates by the distance $\overline{\boldsymbol{PA}} = \boldsymbol{l}$ and the angle $\boldsymbol{\alpha}$. The orientation of the plane of the wheel is characterized by the fixed angle $\boldsymbol{\beta}$. The zero component of the velocity of the contact point is represented by the fixed angle $\boldsymbol{\gamma}$. The rotation angle of the wheel around its axis is denoted by $\boldsymbol{\varphi(t)}$ and the radius is ***r***.

While $\boldsymbol{\delta_m}$ define how many degrees of freedom the robot could have instantaneously without changing its configuration (actual steer angle of the steering wheels), $\boldsymbol{\delta_s}$ define the additional degrees of freedom accessible by steering the wheels.

Hence the total degrees of freedom of the WMR is defined by $\boldsymbol{\delta_M} = \boldsymbol{\delta_m} + \boldsymbol{\delta_s}$.

It follows that only five non-singular structures are of practical interest such that:

- $\boldsymbol{1 \leq \delta_m \leq 3}$

  (mobility cannot exceed the degrees of freedom of the plane while $\delta_m = 0$ means no possible motion)

- $\boldsymbol{2 \leq \delta_M \leq 3}$

  ($\delta_M = 1$ is not acceptable because it corresponds to the rotation of the robot around a fixed instantaneous center of rotation)

- $\mathbf{0 \leq \delta_s \leq 2}$

These five structures present the minimum number of wheels to be classified into that category. Every category can have obviously a bigger number of wheels, but their mobility doesn't change, so for the purpose of classification it has been chosen to use the simplest configuration possible for every kind of structure.

1. $\mathbf{\delta_m = 3, \delta_s = 0}$

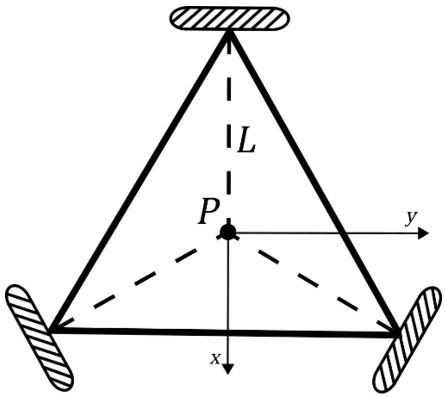

Figure 1.4 Robot of type 3.0

Called Omnidirectional Robot, they don't have conventional fixed or conventional centred wheel but for example three Omni-wheels or three conventional off-centred wheels. Such configuration gives the robot full mobility in the plane and for the one with Omni-wheels this is achieved without any reorientation.

2. $\boldsymbol{\delta_m = 2, \delta_s = 0}$

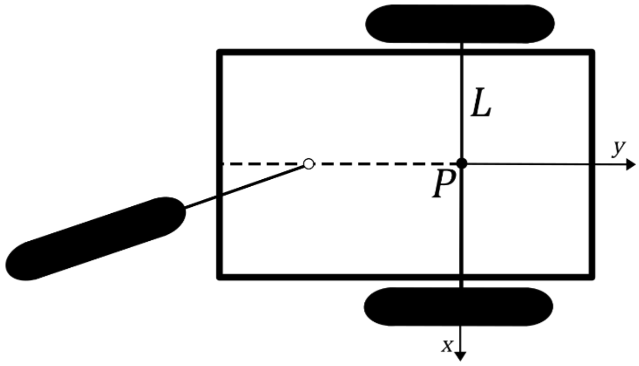

Figure 1.5 Robot of type 2.0

These robots have no conventional centred orientable wheels and either one or several conventional wheels with a single common axle. The velocity results constrained to a two-dimensional distribution. This structure is called “Differential Drive” and is today’s most common used among WMR due to his simple structure and control law.

3. $\boldsymbol{\delta_m = 2, \delta_s = 1}$

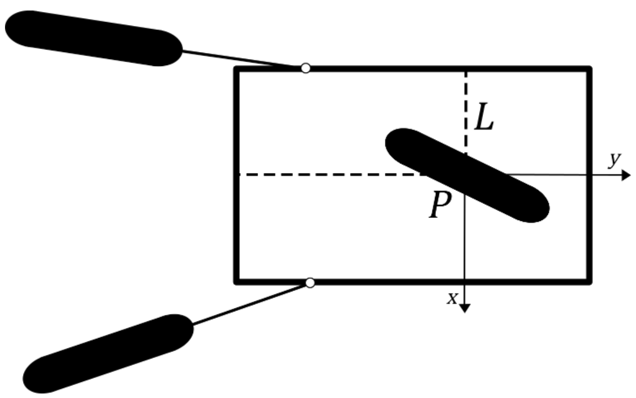

Figure 1.6 Robot of type 2.1

No conventional fixed wheel and at least one conventional centred orientable wheel or more than one but their orientation must be coordinated to maintain $\boldsymbol{\delta_s = 1}$. The velocity results constrained to a two-dimensional distribution.

4. $\boldsymbol{\delta_m = 1, \delta_s = 1}$

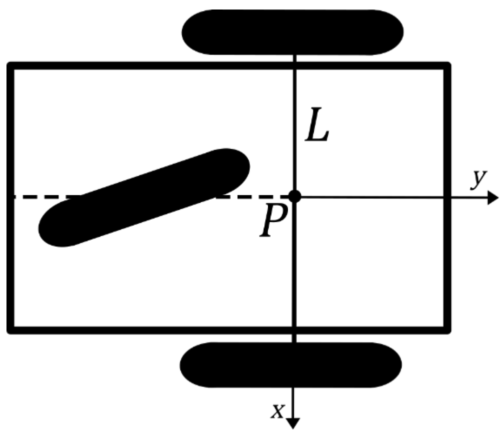

Figure 1.7 Robot of type 1.1

One or several conventional wheels with a single common axle and one or more centred orientable wheels with the conditions that the centre of one of them is not located on the axle of the fixed wheels and their orientation must be coordinated to maintain $\boldsymbol{\delta_s = 1}$. The velocity is constrained to belong to a one-dimensional distribution.

5. $\boldsymbol{\delta_m = 1, \delta_s = 2}$

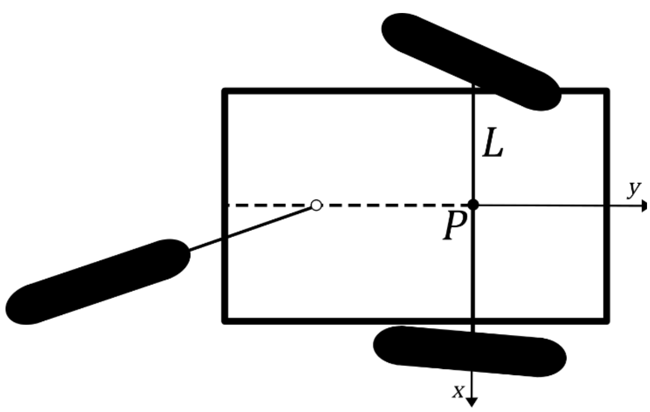

Figure 1.8 Robot of type 1.2

No conventional fixed wheel and at least two conventional centred orientable wheels or more but their orientation must be coordinated to maintain $\boldsymbol{\delta_s = 2}$. The velocity is constrained to belong to a one-dimensional distribution.

1.2 Omnidirectional and pseudo-Omnidirectional robots

For an indoor WMR is important to have $\boldsymbol{\delta_M = 3}$ to maximize the range of movement. As seen before it can be achieved using omni-wheels or conventional wheels. There is a third way as we can see in (6) that "simulate" the 3 DOF. In this example the main body is linked to a differentially driven robot platform by a revolute joint. In this way the "Head" of the WMR has full range of view of the environment even if the platform lack of mobility in the direction orthogonal to the wheels. For this very reason this choice is not preferable because is better having a bit more complex structure that although bring more flexibility to the platform.

WMR with omni-wheels are called, as seen before, omnidirectional and their full mobility without changing configuration allow to follow complex trajectory with a relatively simple mechanical structure because there is no need of steering mechanism. On the other hand the other two structures with $\boldsymbol{\delta_M = 3}$ and conventional wheels are called pseudo-omnidirectional due to the fact that they need to change their configuration (steering the wheels) to achieve full mobility.

Omnidirectional robots seems to have an advantage to pseudo-Omnidirectional ones but, as we can see in (3), (4), (5), the usage of Omni-wheel bring to consistent posture errors due to three big issues affecting this kind of wheel: joint velocity saturation, wheel slippage and perfect actuator synchronization. These posture errors are of big interest because every navigation algorithm needs to compute the WMR position by means of odometry. Hence these issues must be addressed in order to use Omni-wheels in autonomous navigation.

This problem is overcome in (7) by using two offset steered driving wheels and two caster wheels showing impressive Omnidirectional Mobility. The over-actuation (4 motors for 3 Dof) allows high agility to the WMR on the plane as we can see in figure 8 but the trajectory to be planned is not uniquely determined. Nevertheless, a not uniquely determined trajectory is useful in order to optimize the motion of the robot.

Similar results but with a more complex structure are achieved in (8), (9), (10), (11) with the implementation of four centred steered driving wheels on the base. Such motion strategy results to much redundant but allows great position accuracy in order to mount a manipulator on the robot base as we can see in (10) and (11).

1.3 Market

It is important to have a look at what offer the market nowadays in order to develop something really innovative.

MoRo

Figure 1.9 MoRo

MoRo is a human-size assistant robot belonging to type (2,0). It features differential drive and two manipulators with 6 DoF each, linked to a shoulder that can be moved at various height. A stereo camera is mounted on a 2 DoF head. It is equipped with a navigation system based on visual SLAM algorithm. Both IR and ultrasonic sensor are used in an obstacle avoidance algorithm. Can recognize object, face and emotion and implement voice interaction trough an app and WIFI connections.

This is a very advanced assistive robot but in the other hand is not cheap at all, as a matter of fact it results unaffordable for most of the people that can be interested in using this kind of technology.

Pepper

Figure 1.10 Pepper

Pepper show a more anthropomorphic appearance with respect to MoRo although sharing similar features like autonomous navigation, obstacle avoidance algorithm and WIFI and Bluetooth connections. In a different way it doesn’t have SLAM and its shoulder are fixed but implements a touchscreen to interact with user in fifteen different languages.

However, the main difference is the fact that it doesn’t use differential drive but 3 omnidirectional wheels belonging to type (3,0). This structure provides a way greater navigation agility but makes difficult internal odometry due to the slippage of the wheel.

Ipal

Figure 1.11 Ipal

Five microphones are implemented on Ipal to allow sound direction detection. Its motion is based on differential drive belongin to type (2,0) and implement two 5 DoF manipulators. It is provided with a mono camera and a touchscreen. Like previous ones can recognize object, face and emotions but cannot navigate autonomously, essential feature for an assistive robot. Wi-Fi and Bluetooth are also provided.

Zembo

Figure 1.12 Asus Zembo

Zembo is the simplest one. Has differential drive belongin to type (2,0) and is capable of autonomous navigation and obstacle avoidance but doesn't have SLAM. It can recognize object and faces and is capable of voice interaction. Is equipped with a 13 megapixels mono camera, IR sensors, ultrasonic sensors and a touchscreen. It is capable of follow lines and moving small objects, but it isn't implemented with manipulators.

Chapter 2

Task analysis

It is important to perform an accurate task analysis of this robot because it will help defines the robot structure according to what this robot must do. First of all, it must be defined the environment where this robot will operate. This kind of robot find its natural operative environment inside the house as a daily help, but it can be found very useful also inside offices, workshops, laboratory, etc. as a valid assistant to the work. Considering that, the first thing that this robot must be able to accomplish is to manage to follow people autonomously without being of any obstacle and also to be able to deliver a service of any kind.

Inside the section 2.1 the analysis of the person follow task will be carried out, starting from defining the various sub-tasks composing it. The choice for the various components of the robot, both Hardware and Software, will be done according to the various requirements of the sub-tasks.

In the section 2.2 the analysis of the services task will be carried out in a similar way of the section 2.1 with the choice of the components that will results from the requirements of the various sub-tasks.

Inside the section 2.3 it is analysed the modularity of the robot and what that concerns in terms of structures and components.

2.1 Person follow task

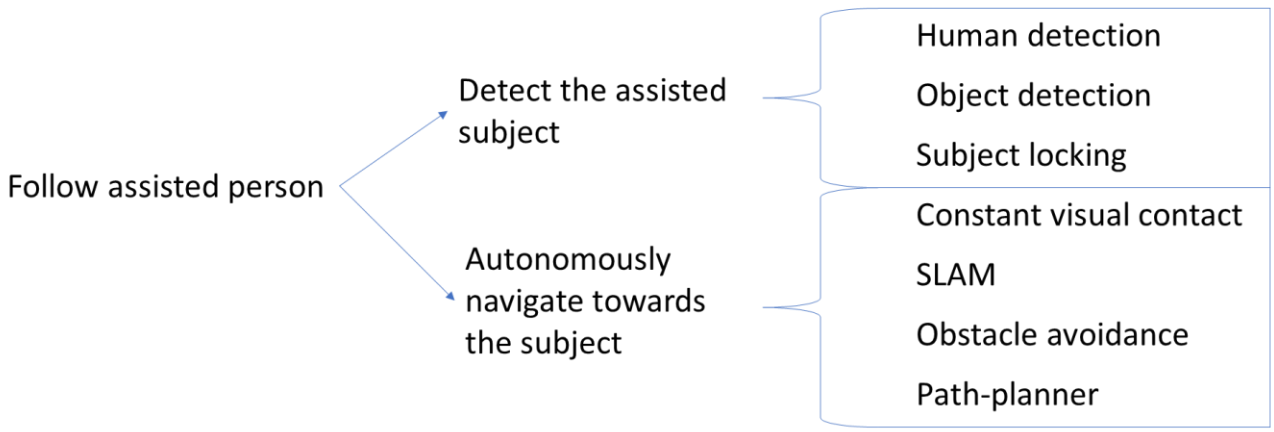

Figure 2.1 Person follow sub-tasks

In order to be able to follow the user, it must detect him and autonomously navigate towards him wherever he goes. Implementing the capability to detect human is therefore fundamental and, moreover, could be improved by a subject locking method. Using object detection functionalities, the robot acquires the ability to block the view on an object, it could be a necklace with led, and recognize the user by it. Could be interesting adding the ability to recognize different users by different necklace.

The basic hardware requirements for both human and object detection is a camera sensor. It must be assembled in a way that could easily maintain constant visual contact with the user even in presence of obstacle obstructing the view. To achieve this, the camera needs to be placed on top of a telescopic pole.
From the Software point of view, a face recognition software is fundamental, as a database in which users face will be stored.

The autonomous navigation needs primarily the SLAM (Simultaneously Localization And Mapping) to be able to locate his position and the position of the user inside the house. Obviously, path-planning functionalities are fundamental to allow the robot to move around. During the movement the WMR needs to avoid unexpected obstacle as a moved chair, a person, a pet, a cable, the stairs, etc.

In addition to the above-mentioned requirements this WMR needs the maximum degree of manoeuvrability possible because it must be able to move around while maintaining constant contact of view with the user. The possible structures that allow that kind of mobility are, as seen in the section 1.1 of this thesis, the Omnidirectional one with three omni wheels and the pseudo omnidirectional one with two steering actuated wheels and on castor wheel. Because the omni wheels bring forth huge positioning errors due to the presence of slippage, the best choice for this robot is the omnidirectional one that allow 3 degree of manoeuvrability and a more accurate localization. To improve stability is recommended to put another castor wheel, so the platform will always lay on almost three wheels during the motion.

This kind of structure needs 2 DC motors to actuate the steering wheels and 2 Stepper motor to steer them. Obviously, every motor needs an appropriate driver to work properly.

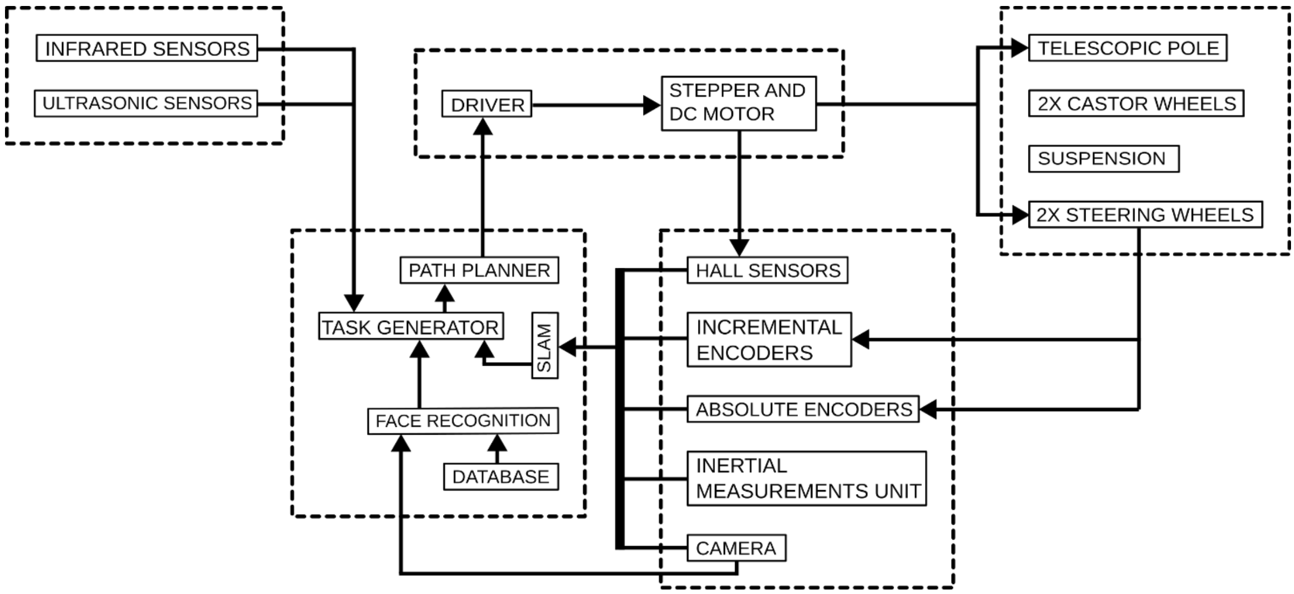

Figure 2.2 Person follow task component choice

To perform the SLAM in an optimal way primarily odometry is computed by means of proprioceptive sensor and then is adjusted trough external measures performed by exteroceptive sensors:

- Incremental encoder to measure wheels speed
- Absolute encoder to measure stepper motor absolute position

- Hall sensor to measure the rotor position and speed of the wheel motors
- Inertial measurements unit to measure acceleration and speed of the robot
- Camera sensor to measure distances from external reference point

Path-planning functionalities are implemented inside the microcontroller that it must be advanced enough to manage these functionalities and the other processes of the robot. Therefore, proximity sensors are fundamental to avoid unexpected obstacle or fall hazard:

- Ultrasonic sensors installed around the perimeter of the platform to detect big obstacles as chair, person, walls etc.
- Infrared sensors installed near the wheels to detect the distance from the ground to avoid the danger of falling from the stairs

A system of suspensions installed on the wheels is fundamental to avoid loss of control in presence of small obstacle as cables on the ground due to an unstable contact wheel-floor.

2.2 Service task

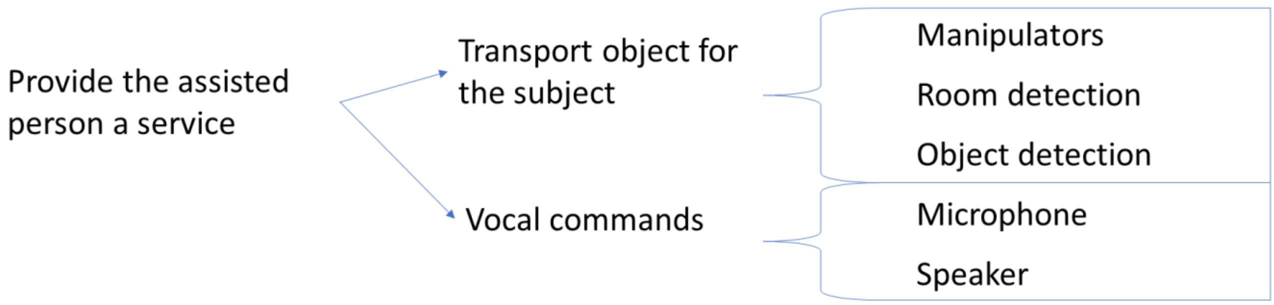

Figure 2.3 Service sub tasks

Useful service that this WMR should provide are fundamentally of two kind:

- Make something in the place of the user in another place of the house
- Provide an intuitive interface to the user
- Giving vocal information when requested

In order to be able to do something in the place of the user, the robot must be able primarily to recognize and localize the various rooms of the house so that it could autonomously go to the place it is asked to. To be able to do so a room detection software is essential, along with a database collecting all the items description useful to classify every room.

After that it must be able to perform the action requested so, due to the fact that most of the task it will be requested to do concern grabbing an object, a small but efficient manipulator is essential along with an object detection software. The above-mentioned manipulator can be simple enough thanks to the chosen structure: a pinch on top of an extendable pole is enough due to the high degree of manoeuvrability of the platform.

The HMI (Human Machine Interface) is fundamental because it is the instrument by means of which the user will be able to use this robot. If it is too much complicate and counter-intuitive the user will not be able to use properly the robot, so it must remain simple and intuitive but in the same time provide all the service the user will need. So beside the obvious choice of the touchscreen a dedicated software will be ned

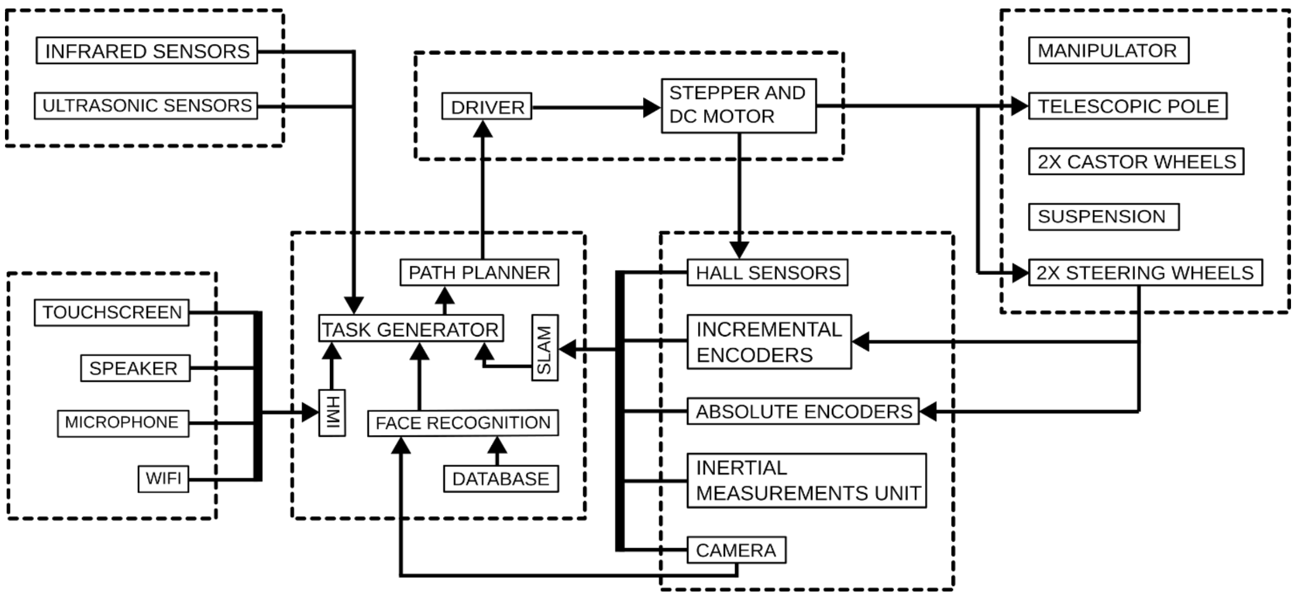

Figure 2.4 Service task component choice

Obviously, a microphone and a speaker are needed to give vocal information and to receive vocal commands, as well as communicate to another person in another room in the place of the user.

Moreover, an internet connection, achievable via Wi-Fi, could be of interest to allow the WMR to answer to the information requested from the user or even contact acquaintance.

2.3 Modularity

Another important feature for this WMR is the modularity. Even if this is not a real task that this robot must be able to accomplish it remain still very useful to analyse because it will affect how its mechatronic layout is structured.

Hence, the robot is splatted in two modules, one is the platform (low-level) with the motion structure and all the sensors related to that and the other is the "head" of the robot (high-level) with the decision-maker software, the human-machine interface and the exteroceptive sensors. This separation allows the two modules to be fully designed autonomously and, most importantly, to be installed with different modules depending on the work situation.

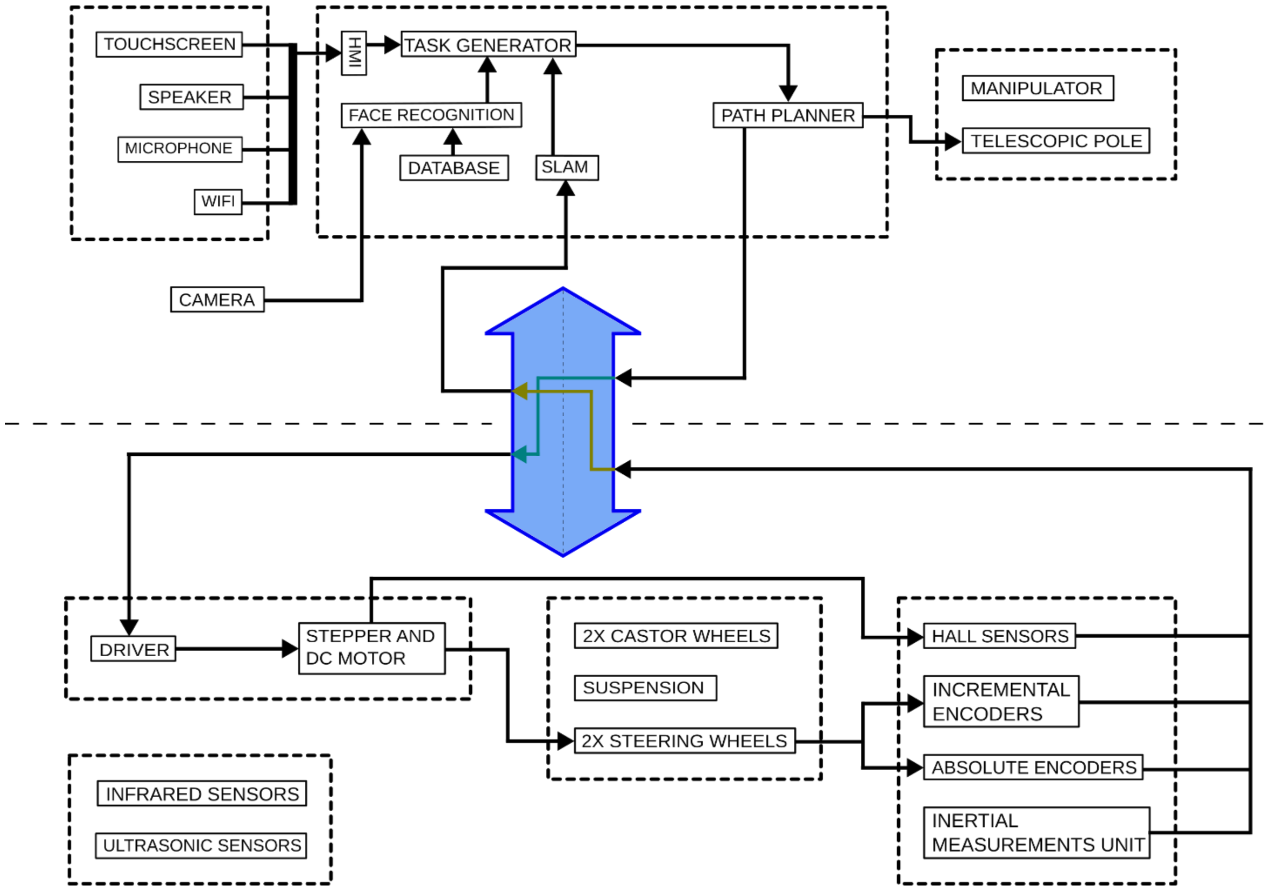

Figure 2.5 Final component choice

These two levels need to communicate between each other: a communication protocol that is able to split completely the two level is of the outmost importance. The communication must be in a way that even if these two modules are connected with other ones it remains the same.

Chapter 3

Kinematic analysis

In this chapter it is carried out the kinematic analysis, that is fundamental in order to understand the motion of this robot.

In the section 3.1 the pose of the platform is defined through the definition of subsequent reference frames. Starting from the reference frame of the chassis, the reference frames of the wheels are defined with a recursive methodology.

In the section 3.2 is defined the generalised speed vectors of the wheels reference frames. Following a similar recursive methodology this speed vector is defined starting from the chassis generalized speed vector.

Inside the section 3.3 the constraint equations are analysed to obtain the relation used to describe the motion of the robot.

In the section 3.4 the direct kinematics is analysed. The relation between the operative space and the joint space is obtained manipulating the constraint equations.

In the section 3.5 the analysis of the inverse kinematic is carried out. At the end of the analysis four possible configurations are defined.

The definition of the centre of instantaneous rotation is defined inside the section 3.6.

Finally, in the section 3.7, four different operative configurations are defined. Each configuration is analysed in order to understand the various behaviour of the platform and how improve the motion of the robot.

3.1 Pose Kinematic

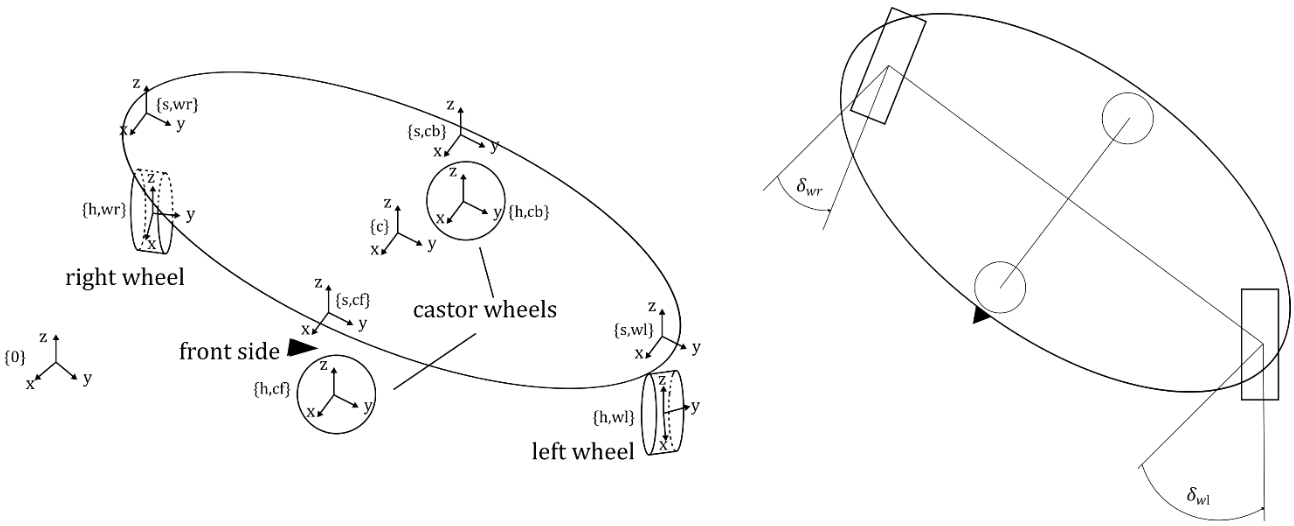

Figure 3.1 Reference frames definition

The pose of the robot can be described completely by a reference frame $\{c\}$, schematised in fig (3.1). Such reference frame is completely defined through the vector ${}^0\underline{p_c} = [x_c, y_c, z_c]^T$, which defines the origin position with respect to the reference frame $\{0\}$ and a 3 angles notation (α, β, γ) with respect to the fixed axes x, y, z of the reference frame $\{0\}$. Transferring such information onto homogeneous notation (which in this document will be denoted as $\hat{R}$), the relation (3.1.1) is obtained.

$$
{}^0\hat{R}_c = \begin{bmatrix} Rot(z,\gamma)Rot(y,\beta)Rot(x,\alpha) & {}^0\underline{p_c} \\ \underline{0}^T & 1 \end{bmatrix} \tag{3.1.1}
$$

Making explicit the relations in equation (3.1.1) the relation (3.1.2) is obtained and by means of that the robot pose results completely defined with respect to the fixed reference frame $\{0\}$.

$$
{}^0\hat{R}_c = \begin{bmatrix} c_\beta c_\gamma & c_\gamma s_\alpha s_\beta - c_\alpha s_\gamma & s_\alpha s_\gamma + c_\alpha c_\gamma s_\beta & x_c \\ c_\beta s_\gamma & c_\alpha c_\gamma + s_\alpha s_\beta s_\gamma & c_\alpha s_\beta s_\gamma - c_\gamma s_\alpha & y_c \\ -s_\beta & c_\beta s_\alpha & c_\alpha c_\beta & z_c \\ 0 & 0 & 0 & 1 \end{bmatrix} \tag{3.1.2}
$$

Where the abbreviated notations c_θ and s_θ stand for $\cos\theta$ and $\sin\theta$.

In order to define the reference frames integral with the chassis and arranged near the attachment points of the wheels, the notation $\{s, \sim\}$ is used where ~ sum up all four frames linked to the wheels, identified by the subscript:

- *wr*: right steering actuated wheel
- *wl*: left steering actuated wheel
- *cf*: front-side castor wheel
- *cb*: back-side castor wheel

The origin position of the reference frames $\{s,\sim\}$ can be easily written inside the reference frame $\{c\}$ defining the constant vectors ${}^{c}\underline{p}_{s,\sim}$, while the orientation is the same as the reference frame $\{c\}$**.** Referring to the parameters defined in fig (3.2), the position of the reference frames $\{s,\sim\}$ is defined by (3.1.3).

$${}^{c}\underline{p}_{s,wr} = [0,-a,0]^T; \qquad {}^{c}\underline{p}_{s,wl} = [0,a,0]^T; \qquad {}^{c}\underline{p}_{s,cf} = [b,0,0]^T; \qquad {}^{c}\underline{p}_{s,cb} = [-b,0,0]^T; \tag{3.1.3}$$

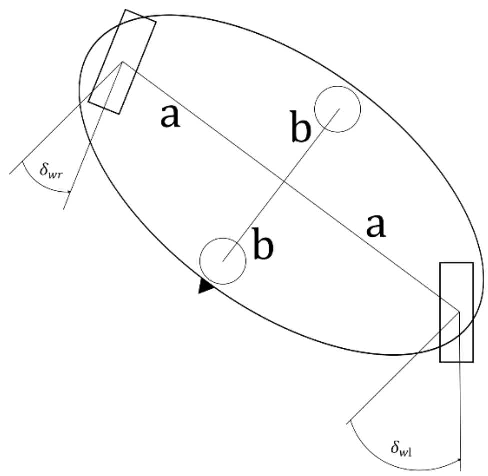

Figure 3.2 Definition of the principal geometric parameters

It follows that the pose of these reference frames is completely defined by the matrix (3.1.4)

$${}^{c}\hat{R}_{s,\sim} = \begin{bmatrix} I_{3x3} & {}^{c}\underline{p}_{s,\sim} \\ \underline{0}^T & 1 \end{bmatrix}; \qquad {}^{0}\hat{R}_{s,\sim} = {}^{0}\hat{R}_{c}\,{}^{c}\hat{R}_{s,\sim} \tag{3.1.4}$$

To proceed with the description of the robot pose, it is useful to introduce the reference frames $\{h,\sim\}$ and $\{w,\sim\}$ whose origin is coincident and is situated on the wheel hub. The orientation of the reference frames $\{h,\sim\}$ with respect to the reference frames $\{s,\sim\}$ is defined by a rotation $\delta_\sim$ around the z-axis of the reference $\{s,\sim\}$ while the frames $\{w,\sim\}$ are obtained, starting by the frames $\{h,\sim\}$, with a rotation $\theta_\sim$ (angle that describes the wheel's rotation around the hub) around the y-axis of the reference frames $\{h,\sim\}$. Therefore, the wheels are characterized by 3 degrees of freedom:

1. A translation $\sigma_\sim$ along the z-axis of $\{s,\sim\}$ allowed by the suspension system
2. A rotation $\delta_\sim$ with respect to the z-axis of $\{s,\sim\}$ allowed by the steering system
3. A rotation $\theta_\sim$ with respect to the y-axis of $\{h,\sim\}$ the wheel's hub

The origin position of the reference frames $\{h\text{-}w,\sim\}$ of the actuated wheels, written with respect to the reference frames $\{s,\sim\}$, are reported on the relation (3.1.5).

$$^{s,wr}\underline{p}_{h,wr} = [0,0,\sigma_{wr}]^T; \qquad ^{s,wl}\underline{p}_{h,wl} = [0,0,\sigma_{wl}]^T \tag{3.1.5}$$

To determine the origin of the reference frames $\{h\text{-}w,\sim\}$ of the passive wheels it must be taken into account of the decentralization b_c along the x-axis of the reference frame $\{h,\sim\}$ due to the typical design of the castor wheels that guarantees the wheel's orientation along the motion direction. Hence, the origin position of the reference frame $\{h\text{-}w,\sim\}$ of the passive wheels are defined by the relation (3.1.6).

$$^{s,cf}\underline{p}_{h,cf} = \begin{bmatrix} 0 \\ 0 \\ \sigma_{cf} \end{bmatrix} + {}^{s,cf}R_{h,cf} \begin{bmatrix} b_c \\ 0 \\ 0 \end{bmatrix}; \qquad ^{s,cb}\underline{p}_{h,cb} = \begin{bmatrix} 0 \\ 0 \\ \sigma_{cb} \end{bmatrix} + {}^{s,cb}R_{h,cb} \begin{bmatrix} b_c \\ 0 \\ 0 \end{bmatrix} \tag{3.1.6}$$

Where $^{s,\sim}R_{h,\sim} = Rot(z,\delta_\sim)$.

The orientation of the reference frames $\{h,\sim\}$, defined with respect to the reference frames $\{s,\sim\}$, is a rotation around the z-axis (coincident with respect to one another) of a steering angle $\delta_\sim$. The orientation of the reference frames $\{w,\sim\}$, defined with respect to the reference frames $\{h,\sim\}$, is a rotation around the y-axis (coincident with respect to one another) of a wheel rotation angle $\theta_\sim$. Summarising, the pose of the reference frames $\{h,\sim\}$ is defined by the homogeneous matrix (3.1.7).

$$^{s,\sim}\hat{R}_{h,\sim} = \begin{bmatrix} Rot(z,\delta_\sim) & ^{s,\sim}\underline{p}_{h,\sim} \\ \underline{0}^T & 1 \end{bmatrix}; \qquad ^0\hat{R}_{h,\sim} = {}^0\hat{R}_{s,\sim}\,{}^{s,\sim}\hat{R}_{h,\sim} \tag{3.1.7}$$

The pose of the reference frames $\{w,\sim\}$ is defined by the homogeneous matrix (3.1.8).

$$^{h,\sim}\hat{R}_{w,\sim} = \begin{bmatrix} Rot(z,\theta_\sim) & \underline{0} \\ \underline{0}^T & 1 \end{bmatrix}; \qquad ^0\hat{R}_{w,\sim} = {}^0\hat{R}_{h,\sim}\,{}^{h,\sim}\hat{R}_{w,\sim} \tag{3.1.8}$$

By means of this recursive procedure, the definition of the reference frames used to describe the kinematic of the robot is completed. Regarding the pose, it is left to define the contact between the wheel and the ground.

3.1.1 Wheel-ground contact model

With an appropriate suspension system, the motion of the robot can be considered almost plane. This consideration introduces a considerable simplification with the robot kinematic. Particularly, it is possible to write the reference frame $\{c\}$ pose, with respect to the reference frame $\{0\}$, by means of the relation (3.1.9).

$$
{}^{0}\hat{R}_{c} = \begin{bmatrix} c_\gamma & -s_\gamma & 0 & x_c \\ s_\gamma & c_\gamma & 0 & y_c \\ 0 & 0 & 1 & z_c \\ 0 & 0 & 0 & 1 \end{bmatrix} \tag{3.1.9}
$$

From which it is obtained ${}^{0}\hat{R}_{h,\sim} = {}^{0}\hat{R}_{c}{}^{c}\hat{R}_{s,\sim}{}^{s,\sim}\hat{R}_{h,\sim}$ and ${}^{0}\hat{R}_{w,\sim} = {}^{0}\hat{R}_{h,\sim}{}^{h,\sim}\hat{R}_{w,\sim}$:

$$
{}^{0}\hat{R}_{h,wr} = \begin{bmatrix} c_{\gamma+\delta_{wr}} & -s_{\gamma+\delta_{wr}} & 0 & x_c + a s_\gamma \\ s_{\gamma+\delta_{wr}} & c_{\gamma+\delta_{wr}} & 0 & y_c - a c_\gamma \\ 0 & 0 & 1 & z_c + \sigma_{wr} \\ 0 & 0 & 0 & 1 \end{bmatrix}; \quad {}^{0}\hat{R}_{h,wl} = \begin{bmatrix} c_{\gamma+\delta_{wl}} & -s_{\gamma+\delta_{wl}} & 0 & x_c - a s_\gamma \\ s_{\gamma+\delta_{wl}} & c_{\gamma+\delta_{wl}} & 0 & y_c + a c_\gamma \\ 0 & 0 & 1 & z_c + \sigma_{wl} \\ 0 & 0 & 0 & 1 \end{bmatrix} \tag{3.1.10}
$$

$$
\begin{gathered}
{}^{0}\hat{R}_{h,wr} = \begin{bmatrix} c_{\theta_{wr}} c_{\gamma+\delta_{wr}} & -s_{\gamma+\delta_{wr}} & s_{\theta_{wr}} c_{\gamma+\delta_{wr}} & x_c + a s_\gamma \\ c_{\theta_{wr}} s_{\gamma+\delta_{wr}} & c_{\gamma+\delta_{wr}} & s_{\theta_{wr}} s_{\gamma+\delta_{wr}} & y_c - a c_\gamma \\ -s_{\theta_{wr}} & 0 & c_{\theta_{wr}} & z_c + \sigma_{wr} \\ 0 & 0 & 0 & 1 \end{bmatrix}; \\
{}^{0}\hat{R}_{h,wl} = \begin{bmatrix} c_{\theta_{wl}} c_{\gamma+\delta_{wl}} & -s_{\gamma+\delta_{wl}} & s_{\theta_{wl}} c_{\gamma+\delta_{wl}} & x_c - a s_\gamma \\ c_{\theta_{wl}} s_{\gamma+\delta_{wl}} & c_{\gamma+\delta_{wl}} & s_{\theta_{wl}} s_{\gamma+\delta_{wl}} & y_c + a c_\gamma \\ -s_{\theta_{wl}} & 0 & c_{\theta_{wl}} & z_c + \sigma_{wl} \\ 0 & 0 & 0 & 1 \end{bmatrix}
\end{gathered} \tag{3.1.11}
$$

Through the simplification of motion almost plane, the pose of the chassis it is defined by 2 position coordinates $(x_c y_c)$ and 1 rotation coordinate (γ). Besides, the suspensions coordinate $\sigma_\sim$ is constant, making simpler the pose of the wheel.

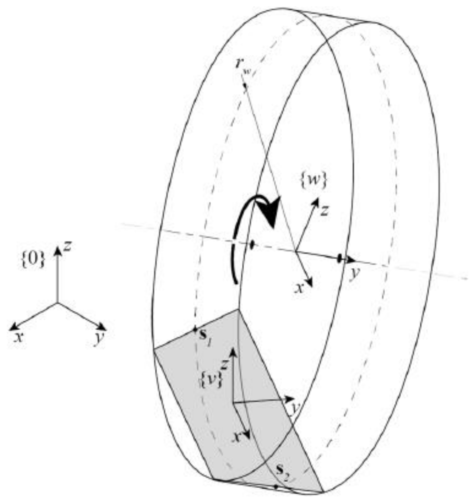

Figure 3.3 Definition of the reference frames for contact points

The position of the four contact points with the ground is coincident with the reference frames $\{h, \sim\}$ projection on the ground. Such contact points are described by the reference frames $\{v, \sim\}$ centered on the contact points. The orientation is easily obtained from the reference frames $\{w, \sim\}$ one observing that:

- The x-axis of $\{v, \sim\}$ lies on the plane x-y of $\{0\}$ and it is directed as the x projection of $\{w, \sim\}$
- The z-axis of $\{v, \sim\}$ is perpendicular to the contact plane and it is parallel to the z-axis of $\{0\}$

In general, the projection of the vector $\underline{u}$ on the plane α passing through the vectors $\underline{v}$ and $\underline{w}$ is given by the relation:

$$\underline{u}_\alpha = \underline{u} - \underline{u}_n = \underline{u} - \frac{\underline{u} \cdot \underline{n}}{\|\underline{n}\|^2}\underline{n}$$

Where $\underline{n}$ is the versor orthogonal to the plane α. On the simplified case of projection on the plane x-y of the reference frame $\{0\}$ it is obtained:

$$^0\underline{u}_\alpha = {^0\underline{u}} - \left({^0\underline{u}} \cdot {^0\underline{k}}\right){^0\underline{k}} = \begin{bmatrix} u_x \\ u_y \\ 0 \end{bmatrix}$$

Hence, it is possible to define the orientation of the reference frames integral to the contact point by means of the relation (3.1.12).

$$
{}^{0}R_{v,\sim} = \begin{bmatrix} \frac{r_{11}}{\sqrt{r_{11}^2+r_{21}^2}} & \frac{r_{21}}{\sqrt{r_{11}^2+r_{21}^2}} & 0 \\ \frac{r_{21}}{\sqrt{r_{11}^2+r_{21}^2}} & \frac{r_{11}}{\sqrt{r_{11}^2+r_{21}^2}} & 0 \\ 0 & 0 & 1 \end{bmatrix} = \begin{bmatrix} c_{\gamma+\delta_{w\sim}} & -s_{\gamma+\delta_{w\sim}} & 0 \\ s_{\gamma+\delta_{w\sim}} & c_{\gamma+\sim} & 0 \\ 0 & 0 & 1 \end{bmatrix} \tag{3.1.12}
$$

Where r_{ij} is the generic element of the matrix ${}^{0}R_{w,\sim}$.

Summarising, the pose of these frames, referred to the reference frame $\{0\}$, is defined by means of the relation (3.1.13).

$$
{}^{0}\hat{R}_{v,wr} = \begin{bmatrix} c_{\gamma+\delta_{wr}} & -s_{\gamma+\delta_{wr}} & 0 & x_c + as_\gamma \\ s_{\gamma+\delta_{wr}} & c_{\gamma+\delta_{wr}} & 0 & y_c - ac_\gamma \\ 0 & 0 & 1 & 0 \\ 0 & 0 & 0 & 1 \end{bmatrix}; \qquad {}^{0}\hat{R}_{v,wl} = \begin{bmatrix} c_{\gamma+\delta_{wl}} & -s_{\gamma+\delta_{wl}} & 0 & x_c - as_\gamma \\ s_{\gamma+\delta_{wl}} & c_{\gamma+\delta_{wl}} & 0 & y_c + ac_\gamma \\ 0 & 0 & 1 & 0 \\ 0 & 0 & 0 & 1 \end{bmatrix} \tag{3.1.13}
$$

For future use, it is useful to obtain the rotation matrix that connect the orientation of the reference frames $\{v, \sim\}$ and $\{w, \sim\}$. Being such matrices orthonormal, the inverse is equal to the transpose. The relations (31.14) results from that.

$$
{}^{v,\sim}R_{w,\sim} = {}^{0}R_{v,\sim}^{T}\,{}^{0}R_{w,\sim} \qquad {}^{w,\sim}R_{v,\sim} = \left({}^{0}R_{v,\sim}^{T}\,{}^{0}R_{w,\sim}\right)^{T} = {}^{0}R_{w,\sim}^{T}\,{}^{0}R_{v,\sim} \tag{3.1.14}
$$

3.2 Velocity kinematic

The velocity of the chassis is described by the generalized speed vector:

$$
\underline{S}_c = \begin{bmatrix} \underline{\omega_c} \\ \underline{v}_c \end{bmatrix} = \begin{bmatrix} \omega_{c,x} \\ \omega_{c,y} \\ \omega_{c,z} \\ v_{c,x} \\ v_{c,y} \\ v_{c,z} \end{bmatrix}
$$

In general, such vector will be completely filled. However only the components $\omega_{c,z} = \dot{\gamma}$, $v_{c,x} = \dot{x}_c$ and $v_{c,y} = \dot{y}_c$ can be controlled inside the operative space. For the purposes of motion planning it is possible to consider null the other components, while such consideration cannot be done for the dynamic modelling. So, it is obtained:

$$\underline{S}_c = \begin{bmatrix} 0 \\ 0 \\ \dot{\gamma} \\ \dot{x}_c \\ \dot{y}_c \\ 0 \end{bmatrix} \tag{3.2.1}$$

The connection points of the suspensions are integral to the frame, so their generalized speed vector is defined by the relation (3.2.2):

$$\underline{S}_{h,\sim} = \begin{bmatrix} \underline{\omega}_c \\ \underline{v}_c + \underline{\omega}_c \times {}^0R_c\,{}^c\underline{p}_{h,\sim} \end{bmatrix} \tag{3.2.2}$$

Especially, for the actuated wheels it is obtained:

$$\underline{S}_{h,wr} = \begin{bmatrix} 0 \\ 0 \\ \dot{\gamma} \\ \dot{x}_c + a\dot{\gamma}c_\gamma \\ \dot{y}_c + a\dot{\gamma}s_\gamma \\ 0 \end{bmatrix}; \qquad \underline{S}_{h,wl} = \begin{bmatrix} 0 \\ 0 \\ \dot{\gamma} \\ \dot{x}_c - a\dot{\gamma}c_\gamma \\ \dot{y}_c - a\dot{\gamma}s_\gamma \\ 0 \end{bmatrix}$$

The hub's velocity with respect to the connection to the frame is described by the vectors:

$${}^{h,wr}\underline{S}_{w,wr} = \begin{bmatrix} 0 \\ 0 \\ \dot{\delta}_{wr} \\ 0 \\ 0 \\ \dot{\sigma}_{wr} \end{bmatrix}; \qquad {}^{h,wl}\underline{S}_{w,wl} = \begin{bmatrix} 0 \\ 0 \\ \dot{\delta}_{wl} \\ 0 \\ 0 \\ \dot{\sigma}_{wl} \end{bmatrix}$$

From which it is possible to write the generalize speed vector for the actuated wheels through the relations (3.2.3).

$$\underline{S}_{w,\sim} = \begin{bmatrix} \underline{\omega}_{h,\sim} + {}^0R_{h,\sim}\,{}^{h,\sim}\underline{\omega}_{w,\sim} \\ \underline{v}_{h,\sim} + {}^0R_{h,\sim}\,{}^{h,\sim}\underline{p}_{w,\sim} \end{bmatrix} \tag{3.2.3}$$

For the purposes of motion planning it is useful considering the system as plane and without suspension on the actuated wheels:

$$\underline{S}_{w,wr} = \begin{bmatrix} 0 \\ 0 \\ \dot{\gamma} + \dot{\delta}_{wr} \\ \dot{x}_c + a\dot{\gamma}c_\gamma \\ \dot{y}_c + a\dot{\gamma}s_\gamma \\ 0 \end{bmatrix}; \qquad \underline{S}_{w,wl} = \begin{bmatrix} 0 \\ 0 \\ \dot{\gamma} + \dot{\delta}_{wl} \\ \dot{x}_c - a\dot{\gamma}c_\gamma \\ \dot{y}_c - a\dot{\gamma}s_\gamma \\ 0 \end{bmatrix}$$

In general, considering the reference frame $\{0\}$ and the reference frame $\{i\}$, which origin is described inside the reference frame $\{0\}$ by the vector ${}^0\underline{p}_i$ and which orientation is defined by the matrix ${}^0R_i$, the position of a point q integral with the reference frame $\{i\}$ can be described as:

$${}^0\underline{p}_q = {}^0\underline{p}_i + {}^0R_i\,{}^i\underline{p}_q \qquad \Rightarrow \qquad {}^i\underline{p}_q = {}^0R_i^T({}^0\underline{p}_q - {}^0\underline{p}_i)$$

Deriving with respect to the time the first one and substituting the second one it is obtained:

$${}^0\dot{\underline{p}}_q = {}^0\dot{\underline{p}}_i + {}^0\dot{R}_i\,{}^0R_i^T({}^0\underline{p}_q - {}^0\underline{p}_i)$$

Comparing the obtained relation with the fundamental formula of the rigid body kinematics the equivalence (3.2.4) is obtained.

$${}^0\dot{R}_i\,{}^0R_i^T = {}^0\omega_i \times \tag{3.2.4}$$

Such relation is useful for the computation of the angular velocity vector of a reference frame starting from its orientation matrix.

Applying the relation (3.2.4) to the reference frames integral with the contact area it is obtained:

$$\omega_{v,\sim} \times = {}^0\dot{R}_{v,\sim}\,{}^0R_{v,\sim}^T \tag{3.2.5}$$

In the case of plain motion can be written as:

$$\underline{\omega}_{v,wr} = \begin{bmatrix} 0 \\ 0 \\ \dot{\gamma} + \dot{\delta}_{wr} \end{bmatrix}; \qquad \underline{\omega}_{v,wl} = \begin{bmatrix} 0 \\ 0 \\ \dot{\gamma} + \dot{\delta}_{wl} \end{bmatrix}$$

In order to obtain the velocity of the reference frames $\{v, \sim\}$ it is possible to write:

$${}^0\dot{\underline{p}}_{v,\sim} = \frac{d}{dt}\left({}^0\underline{p}_{v,\sim}\right) = \frac{d}{dt}\left({}^0\underline{p}_{w,\sim} + {}^0R_{w,\sim}\,{}^{w,\sim}\underline{p}_{v,\sim}\right) \tag{3.2.6}$$

From the equation (3.2.6) it is obtained:

$$ {}^{w,\sim}\underline{p}_{v,\sim} = {}^{0}R^{T}_{w,\sim}({}^{0}\underline{p}_{v,\sim} - {}^{0}\underline{p}_{w,\sim}) \tag{3.2.7} $$

Making explicit the derivative of the equation (3.2.6) e substituting the relation (3.2.7), the relation is obtained:

$$ {}^{0}\underline{\dot{p}}_{v,\sim} = {}^{0}\underline{\dot{p}}_{w,\sim} + {}^{0}\dot{R}_{w,\sim}\left({}^{0}\underline{p}_{v,\sim} - {}^{0}\underline{p}_{w,\sim}\right) = {}^{0}\underline{\dot{p}}_{w,\sim} + {}^{0}\dot{R}_{w,\sim}{}^{0}R^{T}_{w,\sim}\left({}^{0}\underline{p}_{v,\sim} - {}^{0}\underline{p}_{w,\sim}\right) \tag{3.2.8} $$

Deriving the position vectors of the reference frame $\{w, \sim\}$ with respect to the time, the linear speed expressed by the relations (3.2.9) are obtained.

$$ {}^{0}\underline{\dot{p}}_{w,wr} = \begin{bmatrix} \dot{x}_c + a\dot{\gamma}c_\gamma \\ \dot{y}_c + a\dot{\gamma}s_\gamma \\ 0 \end{bmatrix}; \qquad {}^{0}\underline{\dot{p}}_{w,wl} = \begin{bmatrix} \dot{x}_c - a\dot{\gamma}c_\gamma \\ \dot{y}_c - a\dot{\gamma}s_\gamma \\ 0 \end{bmatrix} \tag{3.2.9} $$

Making explicit the product ${}^{0}\dot{R}_{w,\sim}{}^{0}R^{T}_{w,\sim}$ the relation (3.2.10) is obtained.

$$ {}^{0}\dot{R}_{w,\sim}{}^{0}R^{T}_{w,\sim}\left({}^{0}\underline{p}_{v,\sim} - {}^{0}\underline{p}_{w,\sim}\right) = \dot{\theta}_\sim \begin{bmatrix} 0 & 0 & c_{\gamma+\delta_\sim} \\ 0 & 0 & s_{\gamma+\delta_\sim} \\ -c_{\gamma+\delta_\sim} & -s_{\gamma+\delta_\sim} & 0 \end{bmatrix} \begin{bmatrix} 0 \\ 0 \\ -r_w \end{bmatrix} = \begin{bmatrix} -r_w\dot{\theta}_\sim c_{\gamma+\delta_\sim} \\ -r_w\dot{\theta}_\sim s_{\gamma+\delta_\sim} \\ 0 \end{bmatrix} \tag{3.2.10} $$

Summarizing, the generalize speed vectors associated with the reference frames $\{v, \sim\}$ are defined by the relation (3.2.11).

$$ \underline{S}_{v,wr} = \begin{bmatrix} 0 \\ 0 \\ \dot{\gamma} + \dot{\delta}_{wr} \\ \dot{x}_c + a\dot{\gamma}c_\gamma - r_w\dot{\theta}_{wr}c_{\gamma+\delta_{wr}} \\ \dot{y}_c + a\dot{\gamma}s_\gamma - r_w\dot{\theta}_{wr}s_{\gamma+\delta_{wr}} \\ 0 \end{bmatrix}; \qquad \underline{S}_{v,wl} = \begin{bmatrix} 0 \\ 0 \\ \dot{\gamma} + \dot{\delta}_{wl} \\ \dot{x}_c - a\dot{\gamma}c_\gamma - r_w\dot{\theta}_{wl}c_{\gamma+\delta_{wl}} \\ \dot{y}_c - a\dot{\gamma}s_\gamma - r_w\dot{\theta}_{wl}s_{\gamma+\delta_{wl}} \\ 0 \end{bmatrix} \tag{3.2.11} $$

3.3 Constraint equations

In order to respect the pure rolling constraint, the velocity of the contact point must be equal to zero. The constraint on the passive wheels is not useful to the motion planning, while the constraint equation obtained imposing the constraint on the actuated wheels are relevant. Such constraint is translated in a set of 3 equations for every wheel as:

$$^{0}\underline{\dot{p}}_{v,\sim} = \underline{0} \tag{3.3.1}$$

Considering the expressions defined on the equation (3.2.11), the constraint equation (3.3.1), for the two actuated wheels, can be written in the shape (3.3.2).

$$\begin{cases} \dot{x}_c + a\dot{\gamma}c_\gamma - r_w\dot{\theta}_{wr}c_{\gamma+\delta_{wr}} = 0; & (a) \\ \dot{y}_c + a\dot{\gamma}s_\gamma - r_w\dot{\theta}_{wr}s_{\gamma+\delta_{wr}} = 0; & (b) \\ \dot{x}_c - a\dot{\gamma}c_\gamma - r_w\dot{\theta}_{wl}c_{\gamma+\delta_{wl}} = 0; & (c) \\ \dot{y}_c - a\dot{\gamma}s_\gamma - r_w\dot{\theta}_{wl}s_{\gamma+\delta_{wl}} = 0; & (d) \end{cases} \Leftrightarrow \quad \underline{\Phi} = \begin{bmatrix} \dot{x}_c + a\dot{\gamma}c_\gamma - r_w\dot{\theta}_{wr}c_{\gamma+\delta_{wr}} \\ \dot{y}_c + a\dot{\gamma}s_\gamma - r_w\dot{\theta}_{wr}s_{\gamma+\delta_{wr}} \\ \dot{x}_c - a\dot{\gamma}c_\gamma - r_w\dot{\theta}_{wl}c_{\gamma+\delta_{wl}} \\ \dot{y}_c - a\dot{\gamma}s_\gamma - r_w\dot{\theta}_{wl}s_{\gamma+\delta_{wl}} \end{bmatrix} = \underline{0} \tag{3.3.2}$$

From this set of constraint equation, it is possible to obtain a relation useful to understand the true manoeuvrability of the robot. Particularly, subtracting to the equations (3.3.2)(a) and (3.3.2)(b) the equations (3.3.2)(c) and (3.3.2)(d) the equations are obtained:

$$(a) - (c) \Rightarrow 2a\dot{\gamma} = r_w\left(\dot{\theta}_{wr}c_{\delta_{wr}} - \dot{\theta}_{wl}c_{\delta_{wl}}\right) - r_w\frac{s_\gamma}{c_\gamma}\left(\dot{\theta}_{wr}s_{\delta_{wr}} - \dot{\theta}_{wl}s_{\delta_{wl}}\right)$$

$$(b) - (d) \Rightarrow 2a\dot{\gamma} = r_w\left(\dot{\theta}_{wr}c_{\delta_{wr}} - \dot{\theta}_{wl}c_{\delta_{wl}}\right) - r_w\frac{c_\gamma}{s_\gamma}\left(\dot{\theta}_{wr}s_{\delta_{wr}} - \dot{\theta}_{wl}s_{\delta_{wl}}\right)$$

From which the wanted relation (3.3.3) is obtained.

$$\dot{\theta}_{wr}s_{\delta_{wr}} = \dot{\theta}_{wl}s_{\delta_{wl}} \tag{3.3.3}$$

It is important to notice that the relation (3.3.3) is always verified when δ_{wr} and δ_{wl} are equal to zero, while imposes a constraint on the assignment of the angular speeds of the two wheels on the others configurations.

3.4 Direct Kinematics

Being the system over actuated, the four constraint equation are over abundant for the means of the computation of the platform speeds inside the operative space given a joint space velocity set. It follows that a relation between the joint space speeds must exists. Such relation (equation (3.3.3)) is already obtained inside the section 3.3.

In order to obtain the relation between the joint space quantity that can be actuated (wheels space) $\begin{bmatrix}\dot{\theta}_{wr} & \delta_{wr} & \dot{\theta}_{wl} & s_{\delta_{wl}}\end{bmatrix}^T$ and the operative space controllable speeds $[\dot{x}_c \quad \dot{y}_c \quad \dot{\gamma}]^T$ the set of equations (3.3.2) must be reworked keeping into account the relation (3.2.3). it is obtained in this way:

$$(a) + (c) \Rightarrow 2\dot{x}_c = r_w\left(\dot{\theta}_{wr}c_{\gamma+\delta_{wr}} + \dot{\theta}_{wl}c_{\gamma+\delta_{wl}}\right)$$

$$(b) + (d) \Rightarrow 2\dot{y}_c = r_w\left(\dot{\theta}_{wr}s_{\gamma+\delta_{wr}} + \dot{\theta}_{wl}s_{\gamma+\delta_{wl}}\right)$$

$$(a) - (c) \Rightarrow 2a\dot{\gamma} = r_w\left(\dot{\theta}_{wr}c_{\delta_{wr}} - \dot{\theta}_{wl}c_{\delta_{wl}}\right)$$

Relations that can be rewritten with the matrix notation (3.4.1).

$$\begin{bmatrix}\dot{x}_c \\ \dot{y}_c \\ \dot{\gamma}\end{bmatrix} = \frac{r_w}{2}\begin{bmatrix}\dot{\theta}_{wr}c_{\gamma+\delta_{wr}} + \dot{\theta}_{wl}c_{\gamma+\delta_{wl}} \\ \dot{\theta}_{wr}s_{\gamma+\delta_{wr}} + \dot{\theta}_{wl}s_{\gamma+\delta_{wl}} \\ \frac{1}{a}\dot{\theta}_{wr}c_{\delta_{wr}} - \frac{1}{a}\dot{\theta}_{wl}c_{\delta_{wl}}\end{bmatrix} \tag{3.4.1}$$

It is important to note that the angular speed $\dot{\gamma}$ is equal to zero when:

- $\delta_{wr} = \delta_{wr} = \frac{\pi}{2}$ whichever value $\dot{\theta}_{wr}$ and $\dot{\theta}_{wl}$ assumes (due to the relation (3.3.3) they are forced to stay equal between each other)
- $\delta_{wr} = \delta_{wr}$ and $\dot{\theta}_{wr} = \dot{\theta}_{wl}$

When $s_{\delta_{wl}} \neq 0$ or rather $s_{\delta_{wl}} \neq i\pi$, with $i \in \mathbb{Z}$, keeping into account the constraint between the wheels angular speed (relation (3.3.3)), it is possible to rewrite the relations (3.4.1) into the shape (3.4.2).

$$\begin{bmatrix}\dot{x}_c \\ \dot{y}_c \\ \dot{\gamma}\end{bmatrix} = \frac{r_w}{2}\begin{bmatrix}\dot{\theta}_{wr}\frac{s_{\delta_{wr}+\delta_{wl}}c_\gamma - 2s_{\delta_{wr}}s_{\delta_{wl}}s_\gamma}{s_{\delta_{wl}}} \\ \dot{\theta}_{wr}\frac{s_{\delta_{wr}+\delta_{wl}}s_\gamma - 2s_{\delta_{wr}}s_{\delta_{wl}}c_\gamma}{s_{\delta_{wl}}} \\ \frac{\dot{\theta}_{wr}}{a}\frac{s_{\delta_{wr}+\delta_{wl}}}{s_{\delta_{wl}}}\end{bmatrix} \tag{3.4.2}$$

If $s_{\delta_{wl}} = 0$ the wheels angular speeds can assume every value and so it is possible to simplify the relations (3.4.1) obtaining the relation (3.4.3).

$$\begin{bmatrix}\dot{x}_c\\ \dot{y}_c\\ \dot{\gamma}\end{bmatrix} = \frac{r_w}{2}\begin{bmatrix}\dot{\theta}_{wr}c_{\gamma+\delta_{wr}} \pm \dot{\theta}_{wl}c_{\gamma}\\ \dot{\theta}_{wr}s_{\gamma+\delta_{wr}} \pm \dot{\theta}_{wl}c_{\gamma}\\ \frac{1}{a}\dot{\theta}_{wr}c_{\delta_{wr}} \mp \frac{1}{a}\dot{\theta}_{wl}\end{bmatrix} \tag{3.4.3}$$

3.5 Inverse kinematics

To obtain a solution to the inverse kinematic problem (relation that allow to go from the operative space to the joint space) it is possible to work on the constraint relations (equation (3.3.2)) as follows:

$$(a)^2 + (b)^2 \Rightarrow \left(\dot{x}_c + a\dot{\gamma}c_\gamma\right)^2 + \left(\dot{y}_c + a\dot{\gamma}s_\gamma\right)^2 = r_w^2\dot{\theta}_{wr}^2\left(c_{\gamma+\delta_{wr}}^2 + s_{\gamma+\delta_{wr}}^2\right) = r_w^2\dot{\theta}_{wr}^2$$

$$(c)^2 + (d)^2 \Rightarrow \left(\dot{x}_c - a\dot{\gamma}c_\gamma\right)^2 + \left(\dot{y}_c - a\dot{\gamma}s_\gamma\right)^2 = r_w^2\dot{\theta}_{wl}^2\left(c_{\gamma+\delta_{wl}}^2 + s_{\gamma+\delta_{wl}}^2\right) = r_w^2\dot{\theta}_{wl}^2$$

From which the relation (3.5.1) is obtained.

$$\begin{gathered}\dot{\theta}_{wr} = \pm\frac{1}{r_w}\sqrt{\left(\dot{x}_c + a\dot{\gamma}c_\gamma\right)^2 + \left(\dot{y}_c + a\dot{\gamma}s_\gamma\right)^2}\\ \dot{\theta}_{wl} = \pm\frac{1}{r_w}\sqrt{\left(\dot{x}_c - a\dot{\gamma}c_\gamma\right)^2 + \left(\dot{y}_c - a\dot{\gamma}s_\gamma\right)^2}\end{gathered} \tag{3.5.1}$$

The laws for the variables $\delta_\sim$ will only be obtained for the right wheel, however similar relation can be obtained for the left one, of which only the result will be shown. The relations (3.3.2)(a) and (3.3.2)(b) can be rewritten, using the parametric formulas of sin and cosine, into the shape:

$$\dot{x}_c + a\dot{\gamma}c_\gamma = r_w\dot{\theta}_{wr}c_{\gamma+\delta_{wr}} = r_w\dot{\theta}_{wr}\frac{1-t^2}{1+t^2} \qquad (e)$$

$$\dot{y}_c + a\dot{\gamma}s_\gamma = r_w\dot{\theta}_{wr}s_{\gamma+\delta_{wr}} = r_w\dot{\theta}_{wr}\frac{2t}{1+t^2} \qquad (f)$$

Where $t = tan\frac{\gamma+\delta_{wr}}{2}$ with $\gamma + \delta_{wr} \neq \pi + 2k\pi$, with $k \in \mathbb{Z}$.

Obtaining $(i + t^2)$ from (f) and substituting that in (e) the second-grade equation on t is obtained:

$$t^2 + \frac{\dot{x}_c + a\dot{\gamma}c_\gamma}{\dot{y}_c + a\dot{\gamma}s_\gamma}2t + 1 = 0 \quad \Rightarrow \quad t = -\frac{\dot{x}_c + a\dot{\gamma}c_\gamma}{\dot{y}_c + a\dot{\gamma}s_\gamma} \pm \sqrt{\left(\frac{\dot{x}_c + a\dot{\gamma}c_\gamma}{\dot{y}_c + a\dot{\gamma}s_\gamma}\right)^2 + 1}$$

From this relation the solutions shown into the equation (3.5.2) are obtained.

$$\delta_{wr} = -\gamma - 2arctan\left(\frac{\dot{x}_c + a\dot{\gamma}c_\gamma}{\dot{y}_c + a\dot{\gamma}s_\gamma} \mp \sqrt{\left(\frac{\dot{x}_c + a\dot{\gamma}c_\gamma}{\dot{y}_c + a\dot{\gamma}s_\gamma}\right)^2 + 1}\right) = -\gamma - 2arctan\left(\frac{\dot{x}_c + a\dot{\gamma}c_\gamma}{\dot{y}_c + a\dot{\gamma}s_\gamma} - \frac{r_w\dot{\theta}_{wr}}{\dot{y}_c + a\dot{\gamma}s_\gamma}\right) \tag{3.5.2}$$

Similarly, the two solutions (3.5.3) are obtained.

$$\delta_{wl} = -\gamma - 2arctan\left(\frac{\dot{x}_c - a\dot{\gamma}c_\gamma}{\dot{y}_c - a\dot{\gamma}s_\gamma} \mp \sqrt{\left(\frac{\dot{x}_c - a\dot{\gamma}c_\gamma}{\dot{y}_c - a\dot{\gamma}s_\gamma}\right)^2 + 1}\right) = -\gamma - 2arctan\left(\frac{\dot{x}_c - a\dot{\gamma}c_\gamma}{\dot{y}_c - a\dot{\gamma}s_\gamma} - \frac{r_w\dot{\theta}_{wl}}{\dot{y}_c - a\dot{\gamma}s_\gamma}\right) \tag{3.5.3}$$

In relation to the equations (3.5.1), (3.5.2) and (3.5.3), it can be seen that the relations for the right wheel and for the left wheel provide two independent solutions for each wheel. It follows that the inverse kinematics problem of the platform allows 4 possible configurations, defined by the relations shown into the equation (3.5.4).

$$\mathbf{I} = \begin{bmatrix} \dot{\theta}_{wr} = +\frac{1}{r_w}\sqrt{(\dot{x}_c + a\dot{\gamma}c_\gamma)^2 + (\dot{y}_c + a\dot{\gamma}s_\gamma)^2} \\ \delta_{wr} = -\gamma - 2arctan\left(\frac{\dot{x}_c + a\dot{\gamma}c_\gamma}{\dot{y}_c + a\dot{\gamma}s_\gamma} - \sqrt{\left(\frac{\dot{x}_c + a\dot{\gamma}c_\gamma}{\dot{y}_c + a\dot{\gamma}s_\gamma}\right)^2 + 1}\right) \\ \dot{\theta}_{wl} = +\frac{1}{r_w}\sqrt{(\dot{x}_c - a\dot{\gamma}c_\gamma)^2 + (\dot{y}_c - a\dot{\gamma}s_\gamma)^2} \\ \delta_{wl} = -\gamma - 2arctan\left(\frac{\dot{x}_c - a\dot{\gamma}c_\gamma}{\dot{y}_c - a\dot{\gamma}s_\gamma} - \sqrt{\left(\frac{\dot{x}_c - a\dot{\gamma}c_\gamma}{\dot{y}_c - a\dot{\gamma}s_\gamma}\right)^2 + 1}\right) \end{bmatrix};$$

$$\mathbf{II} = \begin{bmatrix} \dot{\theta}_{wr} = -\frac{1}{r_w}\sqrt{(\dot{x}_c + a\dot{\gamma}c_\gamma)^2 + (\dot{y}_c + a\dot{\gamma}s_\gamma)^2} \\ \delta_{wr} = -\gamma - 2arctan\left(\frac{\dot{x}_c + a\dot{\gamma}c_\gamma}{\dot{y}_c + a\dot{\gamma}s_\gamma} + \sqrt{\left(\frac{\dot{x}_c + a\dot{\gamma}c_\gamma}{\dot{y}_c + a\dot{\gamma}s_\gamma}\right)^2 + 1}\right) \\ \dot{\theta}_{wl} = +\frac{1}{r_w}\sqrt{(\dot{x}_c - a\dot{\gamma}c_\gamma)^2 + (\dot{y}_c - a\dot{\gamma}s_\gamma)^2} \\ \delta_{wl} = -\gamma - 2arctan\left(\frac{\dot{x}_c - a\dot{\gamma}c_\gamma}{\dot{y}_c - a\dot{\gamma}s_\gamma} - \sqrt{\left(\frac{\dot{x}_c - a\dot{\gamma}c_\gamma}{\dot{y}_c - a\dot{\gamma}s_\gamma}\right)^2 + 1}\right) \end{bmatrix}$$

(3.5.4)

$$\textbf{III} = \begin{bmatrix} \dot{\theta}_{wr} = +\frac{1}{r_w}\sqrt{\left(\dot{x}_c + a\dot{\gamma}c_\gamma\right)^2 + \left(\dot{y}_c + a\dot{\gamma}s_\gamma\right)^2} \\ \delta_{wr} = -\gamma - 2arctan\left(\frac{\dot{x}_c+a\dot{\gamma}c_\gamma}{\dot{y}_c+a\dot{\gamma}s_\gamma} - \sqrt{\left(\frac{\dot{x}_c+a\dot{\gamma}c_\gamma}{\dot{y}_c+a\dot{\gamma}s_\gamma}\right)^2 + 1}\right) \\ \dot{\theta}_{wl} = -\frac{1}{r_w}\sqrt{\left(\dot{x}_c - a\dot{\gamma}c_\gamma\right)^2 + \left(\dot{y}_c - a\dot{\gamma}s_\gamma\right)^2} \\ \delta_{wl} = -\gamma - 2arctan\left(\frac{\dot{x}_c-a\dot{\gamma}c_\gamma}{\dot{y}_c-a\dot{\gamma}s_\gamma} + \sqrt{\left(\frac{\dot{x}_c-a\dot{\gamma}c_\gamma}{\dot{y}_c-a\dot{\gamma}s_\gamma}\right)^2 + 1}\right) \end{bmatrix};$$

$$\textbf{IV} = \begin{bmatrix} \dot{\theta}_{wr} = -\frac{1}{r_w}\sqrt{\left(\dot{x}_c + a\dot{\gamma}c_\gamma\right)^2 + \left(\dot{y}_c + a\dot{\gamma}s_\gamma\right)^2} \\ \delta_{wr} = -\gamma - 2arctan\left(\frac{\dot{x}_c+a\dot{\gamma}c_\gamma}{\dot{y}_c+a\dot{\gamma}s_\gamma} + \sqrt{\left(\frac{\dot{x}_c+a\dot{\gamma}c_\gamma}{\dot{y}_c+a\dot{\gamma}s_\gamma}\right)^2 + 1}\right) \\ \dot{\theta}_{wl} = -\frac{1}{r_w}\sqrt{\left(\dot{x}_c - a\dot{\gamma}c_\gamma\right)^2 + \left(\dot{y}_c - a\dot{\gamma}s_\gamma\right)^2} \\ \delta_{wl} = -\gamma - 2arctan\left(\frac{\dot{x}_c-a\dot{\gamma}c_\gamma}{\dot{y}_c-a\dot{\gamma}s_\gamma} + \sqrt{\left(\frac{\dot{x}_c-a\dot{\gamma}c_\gamma}{\dot{y}_c-a\dot{\gamma}s_\gamma}\right)^2 + 1}\right) \end{bmatrix};$$

3.6 Centre of instantaneous rotation

Geometrically, the centre of instantaneous rotation $\underline{I}_{cr}$ is located at the intersection of the projection of the wheels rotation axes on the motion plane $z = 0$. The projection of the wheels rotation axes are located along the y-axis of the reference frames $\{v, \sim\}$. It follows that these lines can be described by the relations:

$$\rho_{wr}: \quad \lambda_1 {}^0R_{v,wr}\underline{j} + {}^0\underline{p}_{v,wr}; \qquad \rho_{wl}: \quad \lambda_2 {}^0R_{v,wl}\underline{j} + {}^0\underline{p}_{v,wl};$$

From the which the system of equations is obtained:

$$\lambda_1 \begin{bmatrix} -s_{\gamma+\delta_{wr}} \\ c_{\gamma+\delta_{wr}} \\ 0 \end{bmatrix} + \begin{bmatrix} x_c + as_\gamma \\ y_c - ac_\gamma \\ 0 \end{bmatrix} = \lambda_2 \begin{bmatrix} -s_{\gamma+\delta_{wl}} \\ c_{\gamma+\delta_{wl}} \\ 0 \end{bmatrix} + \begin{bmatrix} x_c - as_\gamma \\ y_c + ac_\gamma \\ 0 \end{bmatrix}$$

The expressions are obtained solving such system:

$$\lambda_1 = 2a \frac{s_{\delta_{wl}}}{s_{\delta_{wl}-\delta_{wr}}} \qquad \lambda_1 = 2a \frac{s_{\delta_{wr}}}{s_{\delta_{wl}-\delta_{wr}}}$$

Once these relations are known, the centre of instantaneous rotation can be computed by means of the relation (3.6.1).

$$\underline{I}_{cr} = \lambda_1 \begin{bmatrix} -s_{\gamma+\delta_{wr}} \\ c_{\gamma+\delta_{wr}} \\ 0 \end{bmatrix} + \begin{bmatrix} x_c + as_\gamma \\ y_c - ac_\gamma \\ 0 \end{bmatrix} = \begin{bmatrix} a \frac{s_{\delta_{wl}} s_{\gamma+\delta_{wr}} + s_{\delta_{wr}} s_{\gamma+\delta_{wl}}}{s_{\delta_{wl}-\delta_{wr}}} + x_c \\ a \frac{s_{\delta_{wl}} c_{\gamma+\delta_{wr}} + s_{\delta_{wr}} c_{\gamma+\delta_{wl}}}{s_{\delta_{wl}-\delta_{wr}}} + y_c \\ 0 \end{bmatrix} \tag{3.6.1}$$

With this formula it is not possible to compute the centre of instantaneous rotation when $\delta_{wr} = \delta_{wl}$, condition that happen when the wheels are parallel with respect to each other. In such configuration it is possible to write:

$$\underline{v}_c = \begin{bmatrix} 0 \\ 0 \\ \dot{\gamma} \end{bmatrix} \times \left(\underline{p}_c - \underline{I}_{cr} \right) = \begin{bmatrix} -\dot{\gamma}\left(y_c - I_{cr,y}\right) \\ \dot{\gamma}\left(x_c - I_{cr,x}\right) \\ 0 \end{bmatrix}$$

From which the relation (3.6.2) is obtained. Such relation is useful for the computation of the centre of instantaneous rotation under the condition of $\delta_{wr} = \delta_{wl}$.

$$\underline{I}_{cr} = \begin{bmatrix} x_c - \frac{v_{c,y}}{\dot{\gamma}} \\ y_c + \frac{v_{c,x}}{\dot{\gamma}} \\ 0 \end{bmatrix} \tag{3.6.2}$$

The problem is obviously singular for $\dot{\gamma} = 0$.

3.7 Operative configurations

The ways the robot can move can be divided in four different steering configurations, schematized in fig (3.4).

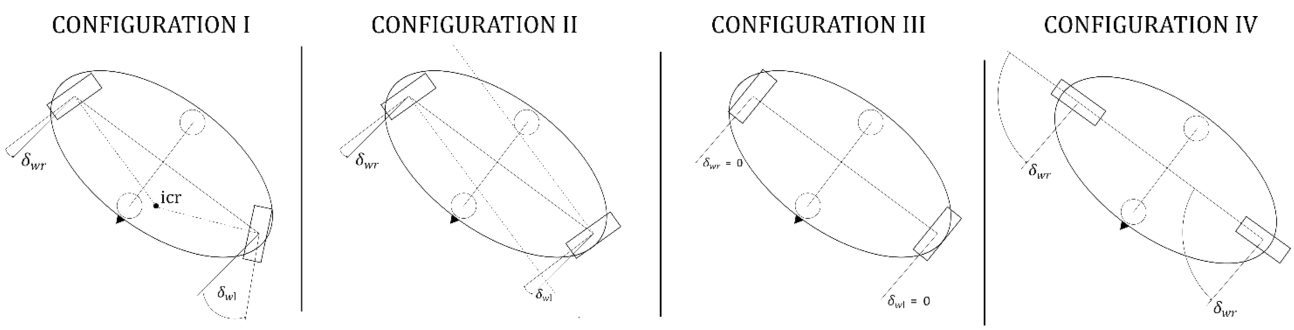

Figure 3.4 Operative configurations

Configuration I $\delta_{wr} \neq \delta_{wl}$. This case represents the most general configuration obtainable, with which the robot can use every grade of mobility to obtain any motion on the plane. The position of the centre of instantaneous rotation is computed with the formula (3.6.1).

Configuration II $\delta_{wr} = \delta_{wl} \neq 0, {}^{\pi}/_{2}$. In this configuration the wheels axes are parallel but not coincident. This configuration allows the robot to translate but not to rotate. As a matter of fact, the equation (3.3.3) impose that the wheels angular speeds must be equal: $\dot{\theta}_{wr} = \dot{\theta}_{wl}$. This kind of configuration can be used, during the person follow task, to maintain a fixed direction of view while translating on the plane.

Configuration III $\delta_{wr} = \delta_{wl} = 0$. This configuration is the classic differential drive: coincident wheels axes. The constraint equation (3.3.3) is always satisfied for any angular speed of the wheels. The position of the centre of instantaneous rotation can be computed with the relation (3.6.2) and it is located on the y-axis of the reference frame $\{c\}$. It follows that the robot can have angular speed, but it loses the possibility to actuate a velocity along the y-axis of $\{c\}$. Such configuration is useful to maintain the centripetal acceleration of the chassis, during curvilinear motion, on the y-axis of $\{c\}$.

Configuration IV $\delta_{wr} = \delta_{wl} = {}^{\pi}/_{2}$. In this configuration, the wheels angular speed must be the same due to the constraint relation (3.3.3) and the wheels axes are parallel, but not coincident. However, this configuration has interesting characteristic from the static and dynamic point of view.

The distances between the two actuated wheels and the two passive wheels are different in order to allow the platform to move into a space built for the humans and filled with obstacle. The robot acceleration around a vertical axis is tied to the capability of its actuators to develop torque around that same axis. It is defined J_{zz} the inertia of the robot around the vertical axis and $F_{h,\sim}$ the resultant force on the chassis owed to the torque application on the wheel $\sim$. Neglecting the forces owed to the passive wheels the relation (3.7.1) is obtained.

$$T_z = a\left(F_{h,wr}c_{\delta_{wr}} - F_{h,wl}c_{\delta_{wl}}\right) = J_{zz}\ddot{\gamma} \qquad \Rightarrow \qquad \ddot{\gamma} = \frac{a}{J_{zz}}\left(F_{h,wr}c_{\delta_{wr}} - F_{h,wl}c_{\delta_{wl}}\right) \quad (3.7.1)$$

From the equation (3.7.1) it is important to notice that the relationship of direct proportionality between the parameter a and the acceleration obtainable along a vertical axis, from which it seems right the choice to put the actuated wheels on the bigger semiaxis of the platform. Furthermore, the platform will sustain in a better way the acceleration along the y-axis with respect to the ones along the x-axis of $\{c\}$. It follows the exigence to maintain the robot acceleration non-parallel to the x-axis.

For this causes the configuration 4 offers the best dynamic resistance to out-of-the-plane solicitation. For this characteristic, the configuration 4 may be used during high-speed motion (for security purposes the robot must be able to stop itself rapidly) and motion with telescopic system extended. This dynamic characteristic is preserved for steering angle inside a small neighbourhood of values centred on $\delta_{wr} = \delta_{wl} = {}^{\pi}/_{2}$. These configurations, although being part of the configuration I, preserve similar dynamic characteristics. It follows the possibility to use these neighbourhoods to approach curvilinear traits keeping the dynamic performances high.

Chapter 4

Trajectory planning

In this chapter is analysed how to develop an optimised method to plan the trajectory for this robot. The trajectory can be defined inside the operative space or inside the joint space, but in the case of a WMR is preferrable to define it inside the operative space to actually control how and where the robot travels inside the workspace. A trajectory inside the operative space is composed by a geometric path, that defines where the robot moves inside the space, and a law of motion that defines how the robot travel along the above-mentioned geometric path.

The parametric definition of the geometric trajectory is carried out inside the section 4.1, first using straight lines and then with Bezier polynomials.

The definition of the motion law is analysed inside the chapter 4.2 for both position and orientation.

4.1 Parametric definition of the geometric trajectory

The most intuitive way to travel inside the operative space from a point A to a point B is with a straight line connecting the various point. Using a parameter k defined inside the interval $0 \leq k \leq 1$, the generic point X is located on the segment as:

$$\underline{p}_X - \underline{p}_A = k\left(\underline{p}_B - \underline{p}_A\right)$$

From which it is obtained the parametric expression of the straight line:

$$\underline{p}_X = (1-k)\underline{p}_A + k\underline{p}_B \quad with \quad 0 \leq k \leq 1 \tag{4.1.1}$$

Deriving the equation (4.1.1) the vectors are obtained:

$$\frac{d}{dk}\left(\underline{p}_X\right) = \left(\underline{p}_B - \underline{p}_A\right); \qquad \frac{d^2}{dk^2}\left(\underline{p}_X\right) = \underline{0}$$

This method appears too rigid because doesn't allow to specify the directions of the tangents on the initial and final points.

However, the straight lines are very useful to defines the parametric variation of the γ:

$$\gamma_X = (1-k)\gamma_A + k\gamma_B \quad with \quad 0 \le k \le 1 \tag{4.1.2}$$

From which is obtained:

$$\frac{d}{dk}(\gamma_X) = (\gamma_B - \gamma_A); \qquad \frac{d^2}{dk^2}(\gamma_X) = 0$$

Using the Bézier polynomials is possible to define parametrically a geometric trajectory between two points through the definition of control points.

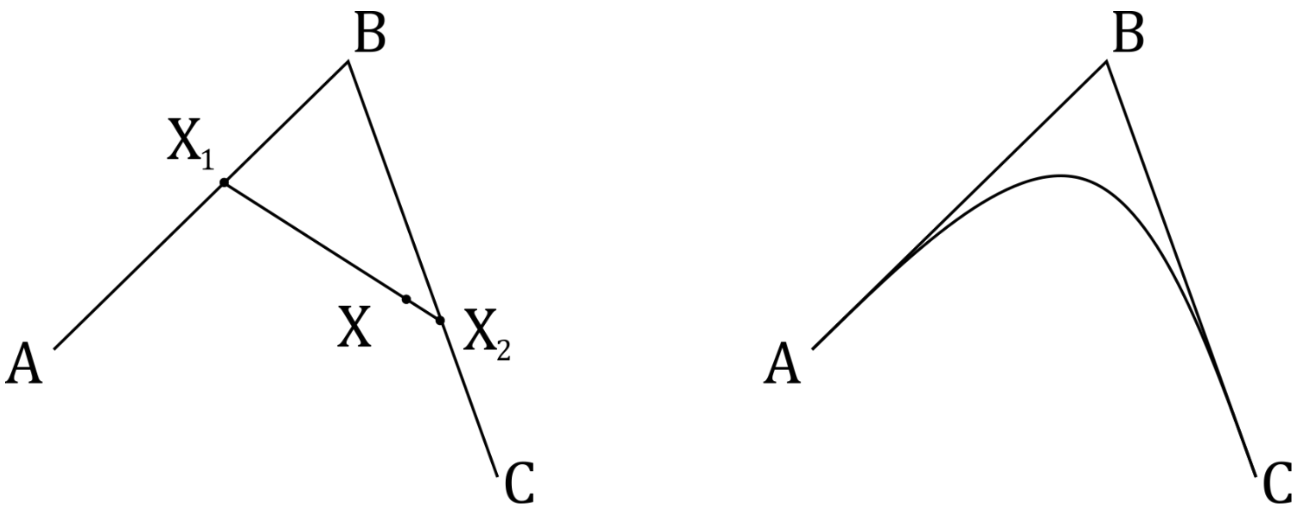

Figure 4.1 Bézier curve with one control point

Considering the figure 4.1, A and C are connected between each other with a regular curve tangent in A to the line AB and tangent in C to the line BC. The generic point X_1 is located on the segment AB and is defined parametrically, using as before the parameter k defined inside the interval $0 \leq k \leq 1$, as:

$$\underline{p}_{X_1} - \underline{p}_A = k\left(\underline{p}_B - \underline{p}_A\right) \Leftrightarrow \underline{p}_{X_1} = (1-k)\underline{p}_A + k\underline{p}_B \quad with \quad 0 \leq k \leq 1$$

Analogously the generic point X_2, located on the segment BC, is defined as:

$$\underline{p}_{X_2} - \underline{p}_B = k\left(\underline{p}_C - \underline{p}_B\right) \Leftrightarrow \underline{p}_{X_2} = (1-k)\underline{p}_B + k\underline{p}_C \quad with \quad 0 \leq k \leq 1$$

Defining the point X as the point of tangency between the line X_1X_2 and the envelop of the lines X_1X_2, it is obtained:

$$\frac{\left|\underline{p}_{X_1} - \underline{p}_X\right|}{\left|\underline{p}_{X_1} - \underline{p}_{X_2}\right|} = \frac{\left|\underline{p}_A - \underline{p}_{X_1}\right|}{\left|\underline{p}_A - \underline{p}_B\right|} = \frac{\left|\underline{p}_B - \underline{p}_{X_2}\right|}{\left|\underline{p}_B - \underline{p}_C\right|} = k$$

From which:

$$\underline{p}_X = (1-k)\underline{p}_{X_1} + k\underline{p}_{X_2} \tag{4.1.3}$$

Substituting inside the (4.1.3) the relations for $\underline{p}_{X_1}$ and $\underline{p}_{X_2}$ it is obtained the parametric expression of the curve between A and C:

$$\underline{p}_X = (1-k)^2\underline{p}_A + 2k(1-k)\underline{p}_B + k^2\underline{p}_C \tag{4.1.4}$$

From which is obtained:

$$\frac{d}{dk}\left(\underline{p}_X\right) = -2(1-k)\underline{p}_A + 2(1-2k)\underline{p}_B + 2k\underline{p}_C$$

$$\frac{d^2}{dk^2}\left(\underline{p}_X\right) = 2\underline{p}_A - 4\underline{p}_B + 2\underline{p}_C$$

It is easy to verify that $\underline{p}_X(0) = \underline{p}_A$, $\underline{p}_X(1) = \underline{p}_C$ and that the tangent in A and C are directed as the segment AB and BC respectively. Such solution remains too rigid, though, because once the control point B is fixed, the tangent in A and C have the direction and the length completely defined.

To obtain a more flexible solution or more precisely a solution that allow to control separately the tangent in the initial and final points a one more control point is needed.

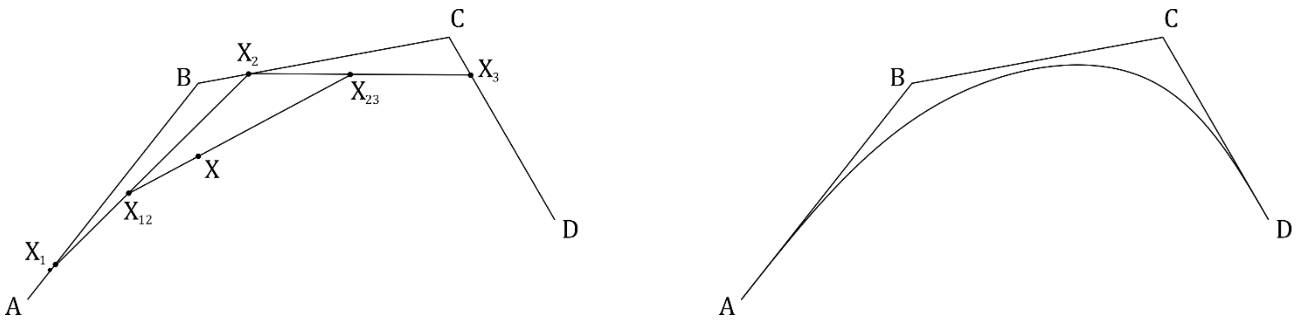

Figure 4.2 Bézier curve with two control points

Referring to the figure 4.2 the parametric expression of the curve is obtained in an analogue way as the problem with only one control point. The generic point X is defined as the point of tangency between the line $X_{12}X_{23}$ and the envelop of the lines $X_{12}X_{23}$. Analogously the point X_{12} and X_{23} are defined using the lines X_1X_2 and X_2X_3 respectively.

First the position of the generic points X_1, X_2 and X_3 are defined using a parameter k, defined in an interval $0 \leq k \leq 1$:

$$\underline{p}_{X_1} - \underline{p}_A = k\left(\underline{p}_B - \underline{p}_A\right) \Leftrightarrow \underline{p}_{X_1} = (1-k)\underline{p}_A + k\underline{p}_B \quad with \quad 0 \leq k \leq 1$$

$$\underline{p}_{X_2} - \underline{p}_B = k\left(\underline{p}_C - \underline{p}_B\right) \Leftrightarrow \underline{p}_{X_2} = (1-k)\underline{p}_B + k\underline{p}_C \quad with \quad 0 \leq k \leq 1$$

$$\underline{p}_{X_3} - \underline{p}_C = k\left(\underline{p}_D - \underline{p}_C\right) \Leftrightarrow \underline{p}_{X_3} = (1-k)\underline{p}_C + k\underline{p}_D \quad with \quad 0 \leq k \leq 1$$

Then the generic points X_{12} and X_{23} are defined in the same way as the relation (4.1.4) is defined:

$$\underline{p}_{X_{12}} = (1-k)^2\underline{p}_A + 2k(1-k)\underline{p}_B + k^2\underline{p}_C$$
$$\underline{p}_{X_{23}} = (1-k)^2\underline{p}_B + 2k(1-k)\underline{p}_C + k^2\underline{p}_D$$

Finally using the same method as before the parametric expression for the generic point X is obtained as:

$$\underline{p}_X = (1-k)^3\underline{p}_A + 3k(1-k)^2\underline{p}_B + 3k^2(1-k)\underline{p}_C + k^3\underline{p}_D \tag{4.1.5}$$

From which are obtained:

$$\frac{d}{dk}\left(\underline{p}_X\right) = -3(1-k)^2\underline{p}_A + 3(1-k)(1-3k)\underline{p}_B + 3k(2-3k)\underline{p}_C + 3k^2\underline{p}_D$$

$$\frac{d^2}{dk^2}\left(\underline{p_X}\right) = 6(1-k)\underline{p_A} - 3(4-3k)\underline{p_B} + 6(1-3k)\underline{p_C} + 6k\underline{p_D}$$

In this way it is possible to obtain a parametric expression of the trajectory for which it is possible to determine the tangent on the initial and final point separately.

4.2 Definition of the motion law

The motion law is defined by simply assigning a time variation law to the parameter k. Such parameter must go from 0 to 1 during a time Δt and have a speed equal to zero in $t = 0s$ and $t = \Delta t$. There are several motion law's shapes that can be picked but the choice must consider some issue:

- In presence of discontinuities of the velocity's law, an infinite value of acceleration is needed and, so, they must be avoided.
- In presence of discontinuities of the acceleration's law there are discontinuities on the actuation of the motors that could cause excessive vibration.
- In presence of a non-zero acceleration value at the end of the motion there could be positioning errors on the final pose of the robot

The most commonly used motion laws are:

- Law with traits at constant acceleration, symmetrical and not
- Biharmonic law
- Cycloidal Law
- Polynomial 3 4 5 law
- Modified trapezoidal law

Knowing the law of time variation of $\underline{p_X}\big(k(t)\big)$ it is possible to compute the velocity's law deriving with respect to the time.

$$\underline{\dot{p}_X} = \frac{d}{dt}\Big(\underline{p_X}\big(k(t)\big)\Big) = \frac{d\underline{p_X}(k)}{dk}\frac{dk(t)}{dt} = \underline{p_X'}(k)\dot{k}(t) \qquad (4.2.1)$$

Deriving once more with respect to the time, the acceleration's law is obtained.

$$\underline{\ddot{p}_X} = \frac{d^2}{dt^2}\Big(\underline{p_X}\big(k(t)\big)\Big) = \frac{d\big(\underline{p_X'}(k)\dot{k}(t)\big)}{dt} = \underline{p_X''}(k)\dot{k}(t) + \underline{p_X'}(k)\ddot{k}(t) \qquad (4.2.2)$$

Analogously as what done for the position, the law of velocity and acceleration for the variable γ are obtained:

$$\dot{\boldsymbol{\gamma}}\big(k(t)\big) = \gamma^{'}(k)\dot{k}(t); \qquad \ddot{\gamma}\big(k(t)\big) = \gamma''(k)\dot{k}(t) + \gamma'(k)\ddot{k}(t) \tag{4.2.3}$$

Chapter 5

Mechatronic design

The choice of the components from the mechatronic point of view of the platform is carried out inside this chapter.

In the section 5.1 there is an overview of all the components inside the platform and how they are connected between each other.

A more detailed view of the connection concerning the wheels motors is described inside the section 5.2 using schematics with point to point connections.

The SPI Bus connections is analysed in the section 5.3, also using schematics with point to point connections.

Analogously in the section 5.4 is described the proximity sensors connections using schematics with point to point connections.

Finally, the problem of the serial interface between High and Low level is addressed inside the section 5.5. A dedicated protocol is defined in order to make the two levels completely independent between each other.

5.1 Generic layout

The first thing to consider when addressing the design of the mechatronic layer of this platform is the modularity. In the chapter (2) it is noted the importance for this platform to be designed separately from the higher layer in order to be employable in different working scenarios and so with different application layer. For example, working in a house with elder people request different service than working in an office.

To make this possible it is essential to have a microcontroller capable to handle autonomously the motion of the platform given the trajectory computed from the application layer and simultaneously collect all the data from the sensors useful to compute the odometry and send them to the application layer. The final choice for the microcontroller is the **Teensy 4.1** a 32-bit Arduino-compatible microcontroller.

To actuate the wheels, it has been chosen the **Maxon EC frameless 45 flat** motor. This is a three-phase brushless motor that occupies a very small amount of space. To have the small encumbrance possible is essential due to the lack of space above the wheels. Moreover, three **Hall sensors** are already installed into this motor, one for each winding.

Maxon also proposes a selection of driver compatible with this motor and so very easy to instal with them. **Maxon ESCON Module 50/5**, the driver chosen, allow, in addition, to handle the Hall sensor installed on the motor and has two analog output to transmit real currents and real rotor position.

To handle these signals an Analog-to-Digital Converter (ADC) is needed. The choice for this device is the **Texas instrument ADS131A04**.

The steering system need to be actuated with the highest accuracy possible, so it is better to use a stepper motor. The chosen device is the **LIN engineering WO-211-20-02**.

The **POLOLU motor driver 36V4** has been chosen to drive the above-mentioned motors. This driver needs to receive set-up data through a SPI interface every time it is turned on so that feature impose the use of a SPI Bus.

In order to maximise the accuracy on the steering angle measurement is essential to install an absolute encoder. Moreover, it must be SPI compatible and so the **Bourns EMS-22** has been chosen.

To improve odometry accuracy an Inertial Measurements Unit (IMU) is introduced. The chosen one is the **Adafruit LSM6DS33** that is Arduino and SPI compatible.

Finally, for the Ultrasonic and Infrared sensor the choice has been made on the **Seeed Grove ULTRASONIC SENSORS** for the first ones and the **SHARP GP2Y0A51SK0F** for the second one.

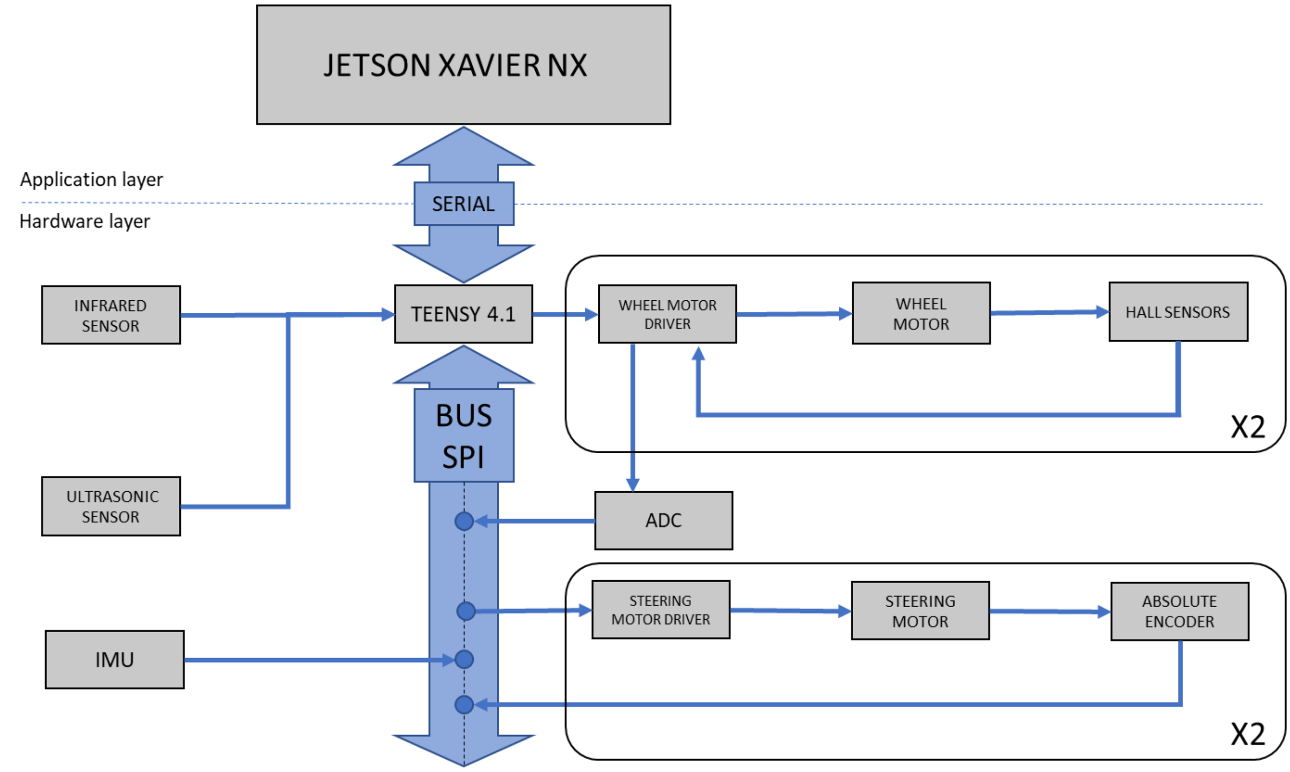

Linea	Segnale
Teensy 4.1 → Escon Module 50/5	PWM
	Abilitazione
	Senso di rotazione
Escon Module 50/5 → Ec Frameless 45	Correnti di controllo
EC Frameless 45→ Hall sensors	Velocità rotori
Hall sensors → Escon Module 50/5	Velocità rotori
Escon Module 50/5 → ADS131A04	Corrente avvolgimenti reale
	Velocità motori reale
Pololu motor driver → WO 211-20-02	
WO 211-20-02→ EMS 22A	Posizione assoluta asse motore
Seeed Ultrasonic sensor → Teensy 4.1	Distanza piattaforma da terreno

Linea			Segnale
SHARP GP2Y0A51SK0F → Teensy 4.1			Presenza di ostacoli in prossimità
SPI Bus	MISO	ADS131A04	Corrente avvolgimenti reale
			Velocità motori reale
		EMS 22A	Posizione assoluta asse motore
		Adafruit LSM6DS33	Accelerazione inerziale
	MOSI	Pololu motor driver	Dati di setup
Serial	→ Hardware layer		Velocità di controllo
			On / Off
	→ Application layer		Dati per calcolo odometria
			Presenza di ostacoli in prossimità
			Status dei componenti

Figure 5.1 Generic Mechatronic Layout

As we can see in figure (5.1) for the communications between application layer and hardware layer a serial connection has been chosen because it allows a fast full-duplex communication between the two devices.

The SPI Bus connect the IMU, the absolute encoder, the ADC and the stepper motor driver to the microcontroller. The infrared and ultrasonic sensors don't need to be putted on the bus because they must warn the microcontroller whenever there is a proximity danger.

5.2 Wheel motor connections

The Escon Module 50/5 can be set up in various way. It has been decided to control the motor's speed via PWM generated by the Teensy 4.1. In addition, an enabling signal is used to allow the motor motion and ii is a digital active high signal. Finally, the sense of rotation is determined by another digital signal: when it is active high the motor will rotate counterclockwise and otherwise it will rotate clockwise. In fig (5.2) the details of the connection between the Teensy 4.1 and the Escon Module 50/5 can be seen.

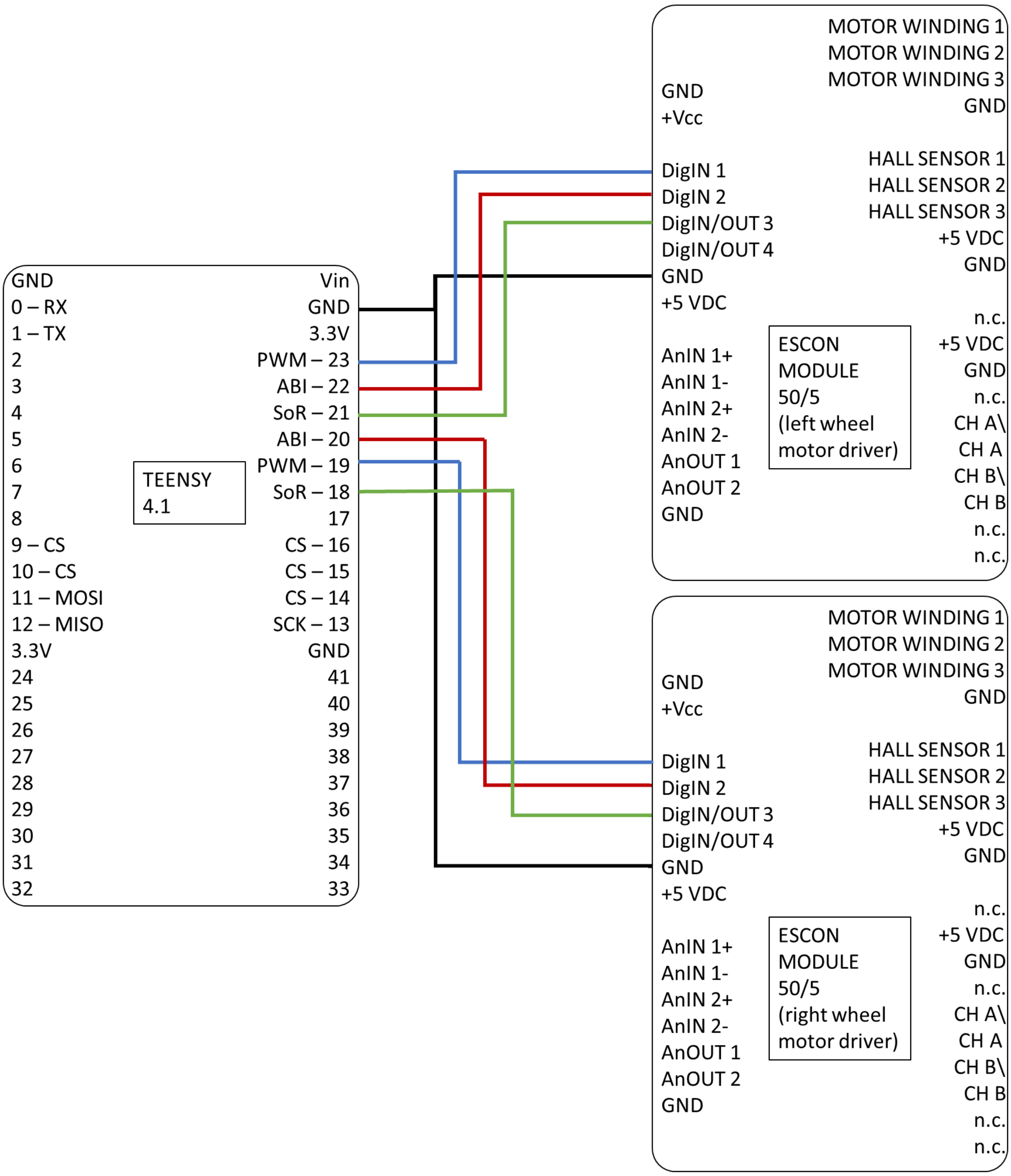

Figure 5.2 Teensy 4.1 -> Escon Module 50/5 connections

Given that the Escon Module 50/5, the motors and the Hall sensors are all from the same manufacturer, Maxon, the connection between each other is standardized. Between driver and motor the cables must be guarder due to the high power values that are transmitted. The driver uses the measurement provided by the hall sensors to close the control loop in speed. In fig (5.3) the details of the connection between the Escon Module 50/5, the motors EC Frameless and the Hall sensors can be seen.

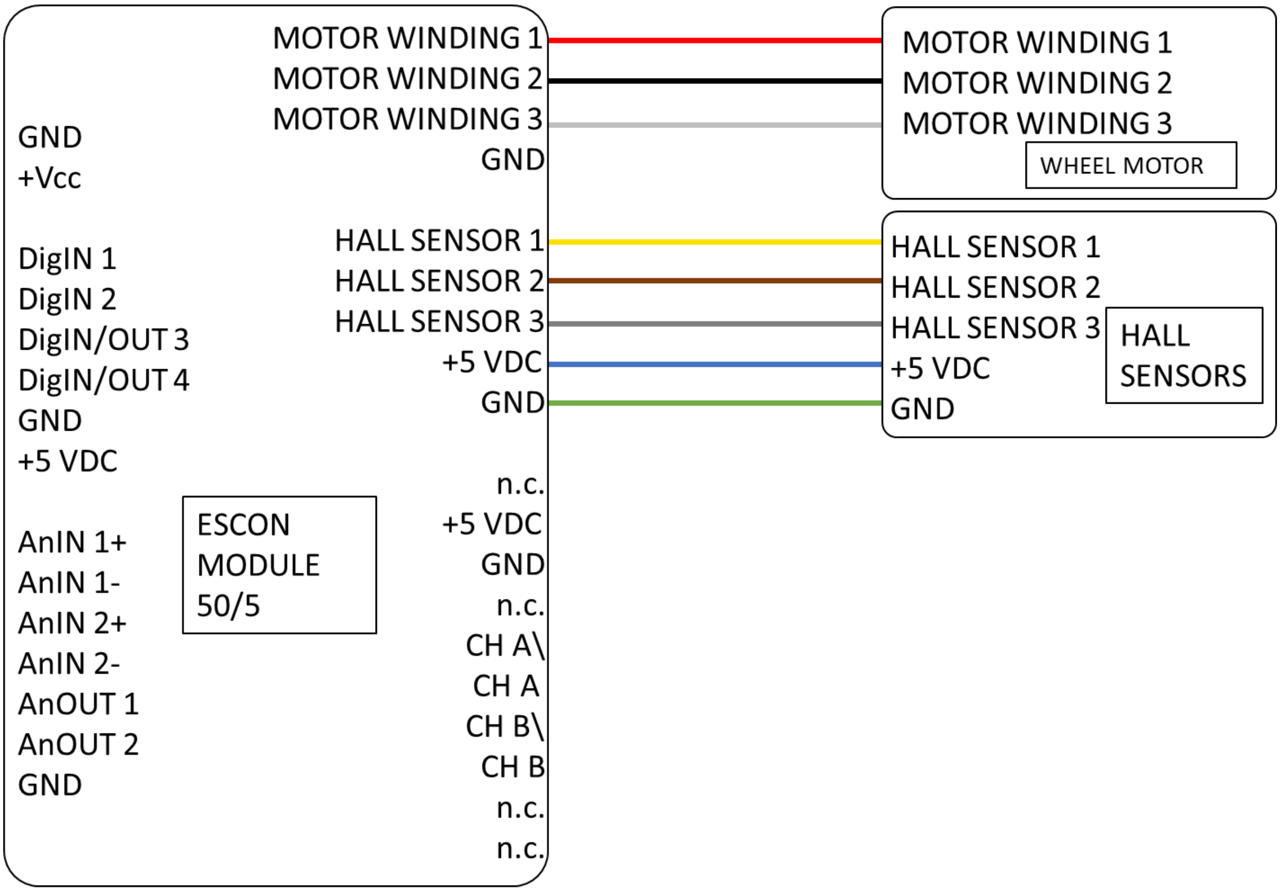

Figure 5.3 Escon module 50/5 -> EC frameless 45 flat connections

The Escon Module 50/5 allow to transmit important measurements through two analog output. The chosen output are the real windings current and the real rotor speed. These two measurements are used to compute the internal odometry of the platform. Because they are analog signals an ADC is needed to convert them into digital signals. In fig (5.4) the details of the connection between the Escon Module 50/5 and the ADC can be seen.

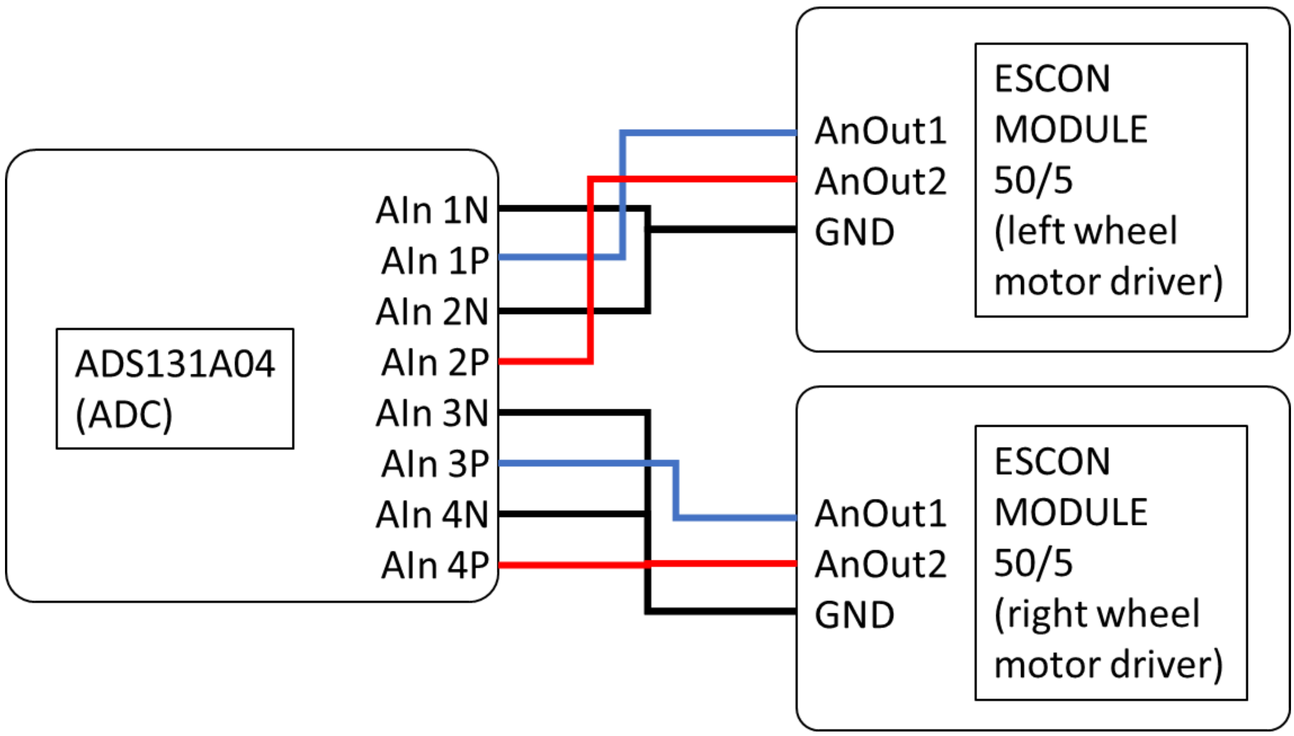

Figure 5.4 Escon Module 50/5 -> ADS131A04 Connections

5.3 SPI Bus

Instead of connecting all the sensors one by one to the microcontroller it has been chosen to use a digital bus in order to reduce the number of cables. For this platform four kind of digital Bus were considered:

- **CAN BUS**: Controlled Area Network, is a digital bus designed for automotive purpose. It has a high noise rejection and can reach a very fats bit rate. The components needed for this kind of bus are a bit oversized for this robot, though.
- **I^{2}C BUS**: Inter Integrated Circuit, is a very simple digital bus designed for projects where simplicity and low manufacturing cost are more important to speed. It has only two lines, besides the reference voltage one, so in terms of number of cables it is very convenient.
- **SPI BUS**: Serial Peripheral Interface, is a very fast digital bus that allow full duplex communication between master and slave. It can be used in a daisy-chain or independent slave configuration. The first one needs only four lines, although it is more than the other two buses, but needs devices specifically designed for this kind of connection while the

independent slave configuration is way faster but the master needs a pin dedicated for every slave in addition to the other lines.

Although an I2C bus would be the best choice to have the smaller number of cables and connections it has been chosen to use an SPI bus due to the need of this kind of bus to set-up the Stepper drivers and so it was pointless to add another digital bus only for the sensors. The preferrable configuration is the independent slave configuration because allow a higher transmission speed and to configure the master-slave connection independently for each slave.

The SPI bus with independent slave configuration has three common lines plus a dedicated one for every slave. Of the three common lines, one is dedicated to the clock, Serial Clock (SCK), and the other two are for data transmission, one is defined Master-Output/Slave-Input (MOSI) and the other one is defined Master-Input/Slave-Output (MISO). The SCK line is used to synchronize every device to the master clock, while the on the other two take place the data transmission. Having two lines dedicated to the data transmission allow a full-duplex communication, the master can send data while receiving data. To select the device with which it wants to communicate, the master uses the above-mentioned slave dedicated line, Chip Select (CS). When the master wants to communicate with one slave it active the CS dedicated to that device and start “talking” while the other devices are not activated. To prevent disturbance on the MISO line all the devices needs a tristate logic connection: when not active this kind of connection assume a high-impedance state, effectively removing the output from the circuit.

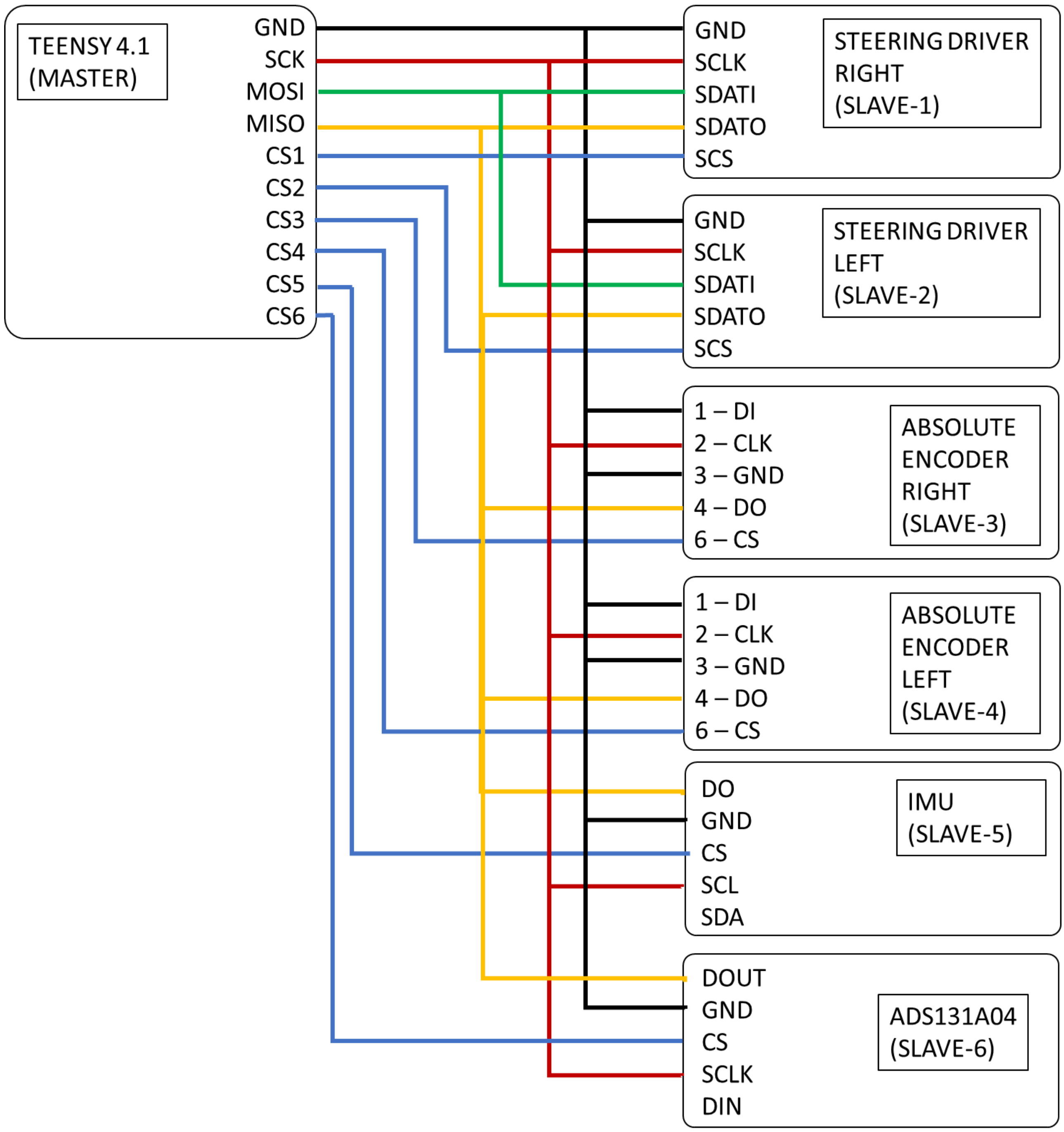

Figure 5.5 SPI Bus Connections

The master device is obviously the Teensy 4.1. The slave devices are the two stepper driver, the two absolute encoder, the IMU and the ADC. The only two devices that receive data on the MOSI line are the stepper drivers and they receive the set-up data as mentioned before. Instead the MISO line is connected to every device on the bus:

- The two stepper drivers send eventual stall detection when microstepping

- The two absolute encoders send the absolute position of the steering shaft
- The IMU send the measured inertial accelerations and speeds
- The ADC send the converted real windings current and real rotor speed of the wheel motors

In fig (5.5) we can see the details of the connection of the SPI bus.

5.4 Proximity Sensors connections

In the environment in which this robot will work not every obstacle can be determined a-priori. As a matter of fact, every kind of unpredicted impediment can occur at every moment during the motion. So, a set of proximity sensors is essential to avoid crash or fall during the motion. It isn't important to put this kind of sensor on the SPI bus because they are not meant to transmit data regularly to the microcontroller, but only in case of imminent danger.

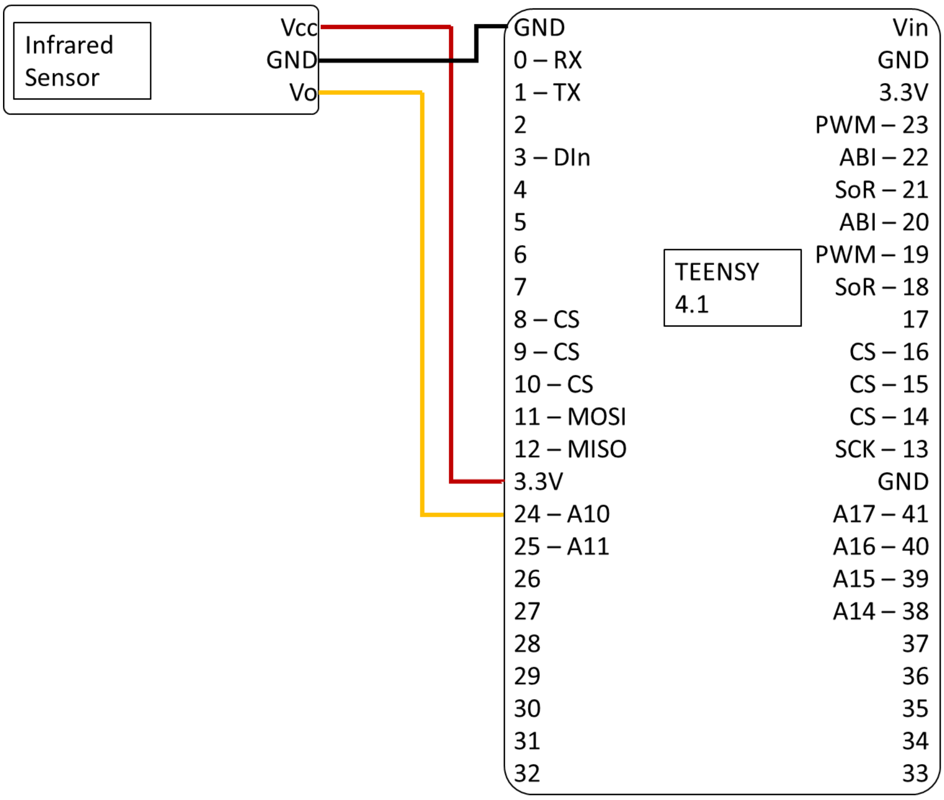

Figure 5.6 Infrared Sensors -> Teensy 4.1 connections

The presence of stairs inside the environment can put in danger of falling the robot. To avoid this issue, infrared sensors are installed in proximity of each wheels to detect whenever the robot is approaching a step. The voltage output of the chosen infrared sensors (SHARP GP2Y0A51SK0F) is proportional to the distance measured in a range of 2-15 cm. In fig (5.6) we can see the details of the connection of the infrared sensors.

To avoid crashes with unpredicted obstacle on the path such as a moved chair or a person, ultrasonic sensors are installed all around the perimeter of the robot. The chosen sensors, GROVE ultrasonic ranger, have a measuring range of 2-350 cm with an angle of 15 degree. The output is PWM with the measured distance proportional to the impulse width. In fig (5.7) we can see the details of the connection of the ultrasonic sensors.

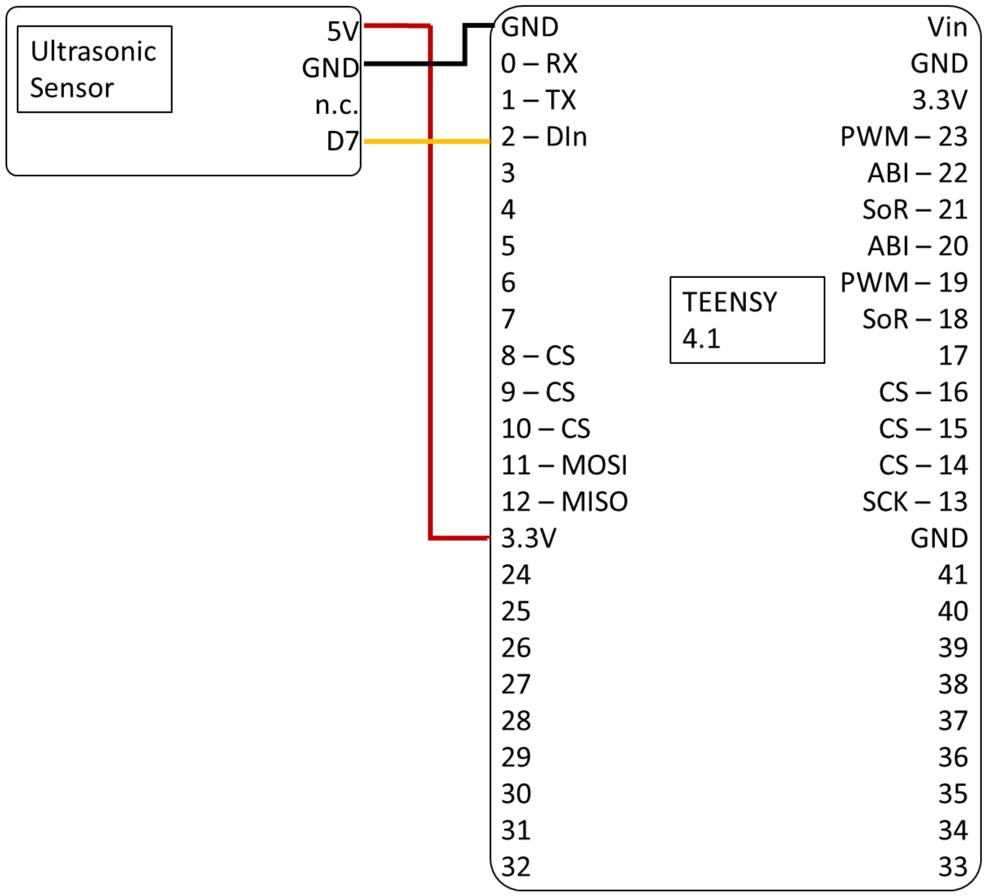

Figure 5.7 Ultrasonic sensors -> Teensy 4.1 connections

5.5 Serial interface

The serial interface is between the hardware layer (HL) and the application layer (AL). It is important to carefully determine what is transmitted between the serial interface because it will condition the modularity of the robot. The serial port of the Teensy 4.1 are TTL level (transistor-transistor logic) so to implement a RS-232 standard connection it is needed a MAX232 conversion chip.

The HL needs to receive from the AL the data used to control the motion of the platform. Such data is represented by the three components of the speed of the cassis that can be controlled in the operative space as said in the section 3.2 of this thesis. These three components are:

- Longitudinal Speed: $v_{c,x} = \dot{x}_c$
- Transverse Speed: $v_{c,y} = \dot{y}_c$
- Yaw Speed: $\omega_{c,z} = \dot{\gamma}$

The choice of this set of speed allow a clear separation between AL and HL. The AL will compute the trajectory knowing only the degree of freedom of the platform without knowing the specific control parameters of the platform used. As a matter of fact, it will be the HL to “translate” the set of speed in the actual control speed for the actuator. Specifically for this platform it is important to notice that all the different configurations are particular cases of the most general one and that the configuration selection is implicit inside the set of speed chosen.

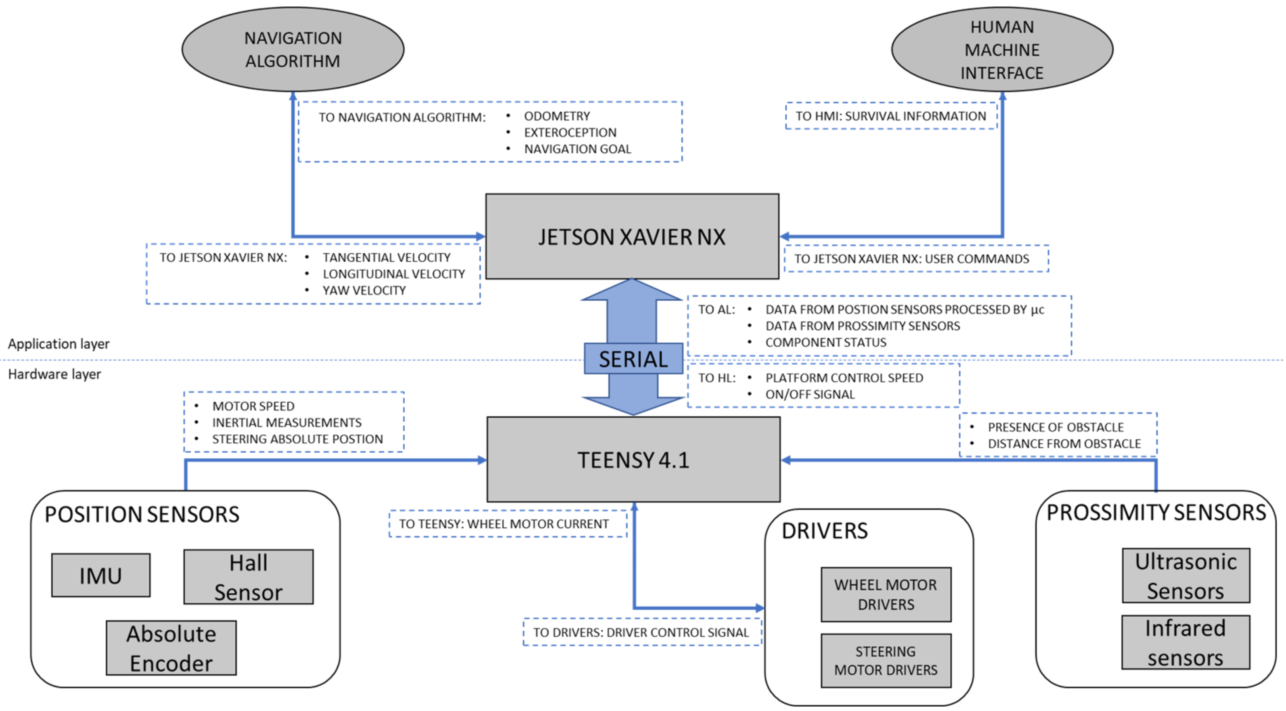

Figure 5.8 Communication Protocol Scheme

Recalling the description of the four configurations in section 3.7, it is important to notice how the value of the speed select implicitly the configuration:

- Configuration I is the most general one, so this configuration is the one that the platform uses whenever the other three are not used.
- Configuration II doesn't allow the robot to translate but not to rotate, so whenever the control yaw speed is equal to zero the configuration that the platform uses is this one.
- Configuration III, also known as Differential Drive, doesn't allow values of speed along the y-axis of $\{c\}$, so whenever the control transverse speed is equal to zero the configuration that the platform uses is the Differential Drive one.
- Configuration IV, also known as Bicycle, doesn't allow values of speed along the x-axis of $\{c\}$, so, like before, whenever the control longitudinal speed is equal to zero the configuration that the platform uses is the Bicycle one.

Summarizing the configuration is chosen from which of the control speed are equal to zero. If two control speed are equal to zero, the robot is either translating along an axis or rotating on the spot, so the chosen configuration is the bicycle one for translation along the y-axis, and the differential drive for translation along the x-axis and for rotation on the spot.

It is important to recall that the bicycle configuration has important dynamic resistance from out-of-the-plane solicitations. This dynamic characteristic is preserved for steering angle inside a small neighbourhood of values centred on $\delta_{wr} = \delta_{wl} = {}^{\pi}/_{2}$. This little steering angle are part of the configuration I and whenever they are used the platform will switch configuration automatically. The risk is that if the AL doesn't know to remain in these little neighbourhood at high speed, not knowing the structure particularities, it can use a set of speed that impose bigger steering angle at high speed causing a safety hazard. This issue can be overwhelmed by an initial instructing phase where the AL "learn" how to control the platform.

On the other directions the AL needs primarily from the HL the necessary data to compute odometry and, so the position if the robot. In order to maintain the modularity, the data sent from the HL must be of the same kind of the control data, hence the AL must receive a set of speed composed of:

- Measured Longitudinal Speed
- Measured Transverse Speed
- Measured Yaw speed

These threes speeds must be computed from the HL microcontroller starting from the data collected from the sensors. In this way the separation between AL and HL is ensured and so they can be designed separately and used with different modules.

Besides that, there are "survival" data that the AL needs to receive to properly control the robot. These survival data are the warnings of the proximity sensors and the status of the HL components. These kinds of data are not meant to be regularly sent over but only when they carry on a warning. So whenever a proximity sensor detects an imminent danger or the microcontroller detects a fault in some component the HL must transmit the information to the AL in order to stop the robot and communicates the fault to the user.

Conclusion and Further Development

In this thesis the initial stages of the design of an assistive robot are analysed. The analysis is focused on building strong basis on which develop a coherent design. As a matter of fact, all the choice made about the design of this robot come out from a process that start at the very beginning with the classification.

Defining those five classes of WMR with respect to their mobility is very helpful in understanding the best structures in relation to the degree of mobility requested from the task of the robot. The final choice concerning the components of the robot is made respecting the requirements came out from the analysis of the various tasks that it must be able to perform. Approaching the design in this way make the process a lot easier because every choice is a natural consequence of what this robot is requested to do.

The final structure of this robot has two driven wheels and two castor wheels, to maximise stability and mobility on the plane. In addition is introduced an important feature for this robot: the modularity. This feature will allow a very high work field flexibility resulting in more appeal to the buyer.

Once the mechanical structure is defined the kinetic analysis has been carried out to understand fully the relation between the operative space and the joint space of this robot. It came out four different operative configurations, each one with pros and cons that have been analysed as well, in order to determine for every kind of motion which configuration is best at.

The way found to plan the trajectory of this robot is by using a Bézier polynomial with two control points for the position and for the γ variable a straight line. In this way the tangent on the initial and final point of the trajectory can be determined separately as the orientation on the plane can be planned independently with respect to the position. It has been seen also how to implement a law of motion with a geometric trajectory.

In the last chapter it is analysed the mechatronic layout in order to satisfy all the requirements, especially for the modular feature. Using the kinematic analysis, a communication protocol that allow a complete separation between high and low level is defined.

As a further development could be of interest developing various modules for various environment of work. For example, the necessities of an office are different from the necessities of a house. So, starting from the definition of the task needed by all the different work environment it is interesting to develop various modules responding to those requirements.

References

1. **United Nations, Department of Economic and Social Affairs.** "World Population Ageing 1950-2050". *United Nations Publications.* 2001.

2. **Campion, G.** "Structural Properties and Classification of Kinematic and Dynamic Models of Wheeled Mobile Robots". *IEEE Trans. Robot. Automat.* 1996.

3. **Han, K. L.** "The source of Position Errors of Omni-directional Mobile Robot with Mecanum Wheel". *IEEE.* 2010.

4. **Indiveri, G.** "Swedish Wheeled Omnidirectional Mobile Robots: Kinematics Analysis and Control". *IEEE Trans. Robot.* 2009.

5. **F. G. Pin.** "A New Family of Omnidirectional and Holonomic Wheeled Platforms for Mobile Robots". *IEEE Trans. Robot. Autom.* 1994.

6. **Jung, M. J.** "Omni-directional Mobile Base OK-II". *IEEE Intern. Confer. Robot. Automat.* 2000.

7. **Wada, M.** "Holonomic and Omnidirectional Vehicle with Conventional Tires". *IEEE Intern. Conf. Robot. Automat.* 1996.

8. **Lauria, M.** "Design and Control of a Four Steered Wheeled Mobile Robot". *IEEE.* 2006.

9. **Hua, F.** "Mechanical Design of a Four-wheel Independent Drive and Steering Mobile Robot Platform". *IEEE.* 2016.

10. **Gurol, B.** "Mechanical and Electrical Design of a Four-Wheel-Drive, Four-Wheel-Steer Manipulator with PA-10 Arm". *IEEE.* 2007.

11. **Reiser, U.** "Care-O-bot 3 - Creating a product vision for service robot applications by integrating design and technology". *IEEE/RSJ Intern. Conf. Intel. Robots Systems.* 2009.

Ringraziamenti

Ringrazio in primo luogo la mia famiglia, che senza il loro perenne supporto non sarei mai riuscito ad arrivare in fondo a questo percorso di studi.

Un enorme ringraziamento a Luca, colui che mi ha sostenuto e guidato in quest’ultimo periodo nella stesura di questa Tesi, senza di lui sarei molto probabilmente ancora al titolo.

Un ringraziamento al Politecnico di Torino che mi ha fatto capire cosa significhi essere un’eccellenza del panorama Universitario mondiale.

Un ringraziamento soprattutto ai miei amici di Torino e Pistoia, su cui ho potuto e potrò sempre contare sia nel bisogno che nel divertimento.

Infine il ringraziamento più grande lo voglio riservare a Silvia, su cui non ho bisogno di spendere altre parole perchè lei sa quanto sia stata fondamentale nel farmi arrivare a questo punto.